University of Natural Resources and Life Sciences, Vienna
Department of Civil Engineering and Natural Hazards
Institute of Mountain Risk Engineering

Master Thesis

Flow Behaviour of Snow in a Rotating Drum

presented by

Kilian Heil

submitted to

BOKU University of Life Sciences and Natural Resources, Vienna

Department of Civil Engineering and Natural Hazards

Institute for Mountain Risk Engineering

Supervisor

Ass. Prof. Dr. Ingrid Reiweger

Assessor

Assoc. Prof. Dr. Roland Kaitna

Vienna, October 2017

Declaration of academic honesty

I certify that the master thesis at hand is to the best of my knowledge and belief the result of my own investigations and is composed by myself unless stated otherwise in the text. All content derived from the work of others has been specifically acknowledged. Furthermore, I confirm that I have not submitted this master thesis either nationally or internationally in any form.

Acknowledgements

I would like to express my very great appreciation to Ingrid Reiweger for her professional guidance, valuable critique, and her encouragement to present my research to an audience of experts. Equal thanks go to Roland Kaitna for his help to operate the rotating drum and his constructive suggestions that enabled me to successfully conduct the experiments.

My gratitude also extends to Martin Falkensteiner and Friedrich Zott for their technical support, as well as to David Prenner for readily helping me with the data analysis, and Jan-Thomas Fischer for contributing his expertise in avalanche dynamics.

A warm thanks to my parents for offering me the possibility to go to university and complete my study with this work.

Finally a very special thanks to Miriam Huber for her infinite patience, outstanding support, and wisdom she provided me with in the last year while I was working on this thesis.

Thank you!

Abstract

Avalanches represent a severe hazard in mountain regions. Although extensive research has been put into the investigation of avalanches, neither their triggering nor their flow behaviour along the transit path are entirely understood. Contributing to avert the danger that comes from avalanches, this work tests a new investigation method for the flow behaviour of snow. A continuous movement of snow in a vertically rotating drum with a diameter 2.5 m and a rectangular cross section of 0.45 m was created. The experimental setup allowed to measure the temperature of the snow and the ambient air, the flow geometry, the basal normal stress distribution, and the volumetric liquid water content over time. In total 13 experiments have been conducted in a temperature range between − 5 ℃ and + 10 ℃ at rotational speeds of 5.2 rpm to 15.2 rpm. Considerable changes in the flow behaviour of the snow such as the onset of granulation and the formation of free liquid water were particularly pronounced at temperatures above − 1 ℃. Moreover the experiments showed that the temperature of the snow could significantly exceed the ambient air temperature if the flowing lobe moved fast enough. The rotating drum constitutes an applicable technique to investigate the flow behaviour of snow. Future research could concentrate on a comprehensive consideration of the energy balance of the flow to enhance physical modelling and improve simulation programs.

German Abstract

Lawinen stellen eine ernst zu nehmende Gefahr in alpinen Regionen dar. Obwohl sich die Wissenschaft intensiv mit Lawinen beschäftigt sind deren Auslösung und das Fließverhalten entlang der Sturzbahn noch nicht vollständig erforscht. Die vorliegende Arbeit stellt eine neue Methode zur Untersuchung des Fließverhaltens von Schnee vor, und soll damit einen Beitrag dazu leisten die Gefahr, welche von Lawinen ausgeht abzuwenden. In einer vertikal rotierenden Trommel mit 2.5 m Durchmesser und einem rechteckigen Fließquerschnitt mit 0.45 m Breite wurde ein gleichmäßiges Fließen von Schnee erzeugt. Der Aufbau des Experiments erlaubte es die Temperatur des Schnees und der Umgebungsluft, das Längsprofil des fließenden Materials, die Normalspannung an der Grundfläche, und den volumetrischen Wassergehalt des Schnees zu messen. Insgesamt wurden 13 Experimente bei Umgebungstemperaturen zwischen -5 ℃ und $+10$ ℃ mit Umdrehungsgeschwindigkeiten von 5.2 U/min bis 15.2 U/min durchgeführt. Bedeutende Änderungen im Fließverhalten wie die der Beginn von Kornbildung und die Bildung von freiem flüssigen Wasser wurden besonders ab Temperaturen oberhalb von -1 ℃ beobachtet. Darüber hinaus zeigten die Experimente, dass die Temperatur des fließenden Schnees deutlich über die Umgebungstemperatur stieg, wenn sich das Material schnell genug bewegte. Die vertikal rotierende Trommel stellt eine geeignete Technik dar, um das Fließverhalten von Schnee zu untersuchen. Weitere Forschungen könnten sich auf eine umfassende Betrachtung der Energieströme konzentrieren um die physikalische Modellierung und Simulationsprogramme weiter zu entwickeln.

Contents

1 Introduction

Avalanches are a severe hazard in alpine regions. People built defence structures from the early 19^{th} century to protect themselves, but they were never able to eliminate the avalanche danger entirely. Contributing to avert the danger that comes from avalanches and to improve the understanding of the physical processes in an avalanche flow, this work presents a new investigation method for the flow behaviour of snow.

Snow moving in an avalanche underlies the influence of continually changing internal properties and external conditions. Particularly the snow properties such as temperature, density, and liquid water content affect the flow behaviour of the moving snow. The physical properties are strongly related to each other, but their interdependency is not yet thoroughly investigated. A way to improve the understanding of avalanche dynamics is to conduct experiments with flowing snow. Basically this can be done in the field or in the laboratory.

On the one hand a suitable hill-slope in the field can be selected and experiments carried out there. The main advantage is that all the tests are correct in geometric scale and time scale. A huge drawback is that the occurring pressures can reach peak values above 1000 kPa (McClung and Schaerer, 2006; Sovilla et al., 2008). Even reinforced concrete is not able to withstand pressures that high. Another disturbance comes from the fact that the experiments in the field are hard to reproduce. A lot of properties like stratigraphy of the snow pack, release volume, entrainment, and atmospheric conditions can not really be controlled.

On the other hand experiments can also be conducted in an indoor or outdoor facility. For example various studies have been done with chutes (e.g. Kern et al., 2004; Schaefer and Bugnion, 2013). In chutes not only the physical properties of the investigated material like density and temperature can be controlled, but also the external effects along the flow path like entrainment and basal roughness can be handled very well. However, the experiments suffer from a small time scale and therefore only represent the dynamic transformation of snow in an avalanche poorly.

Within this thesis I work with a rotating drum that allows not only to investigate the dynamic transformation of the snow at controlled boundary conditions, but also provides data continuously for any time scale.

1.1 Research questions

The research questions of this thesis can be summarized with:

- What are the relevant experimental properties and how do they influence what is observed in the experiments?
- How do the flow quantities evolve during time?
- Is there some direct connection between the temperature evolution of the snow and the onset of granulation?
- Is there some direct connection between the liquid water content and onset of granulation?

1.2 Liquid water in snow

Liquid water in the snow has its source either in rain, melt or a contribution of both. At temperatures at 0 ℃ liquid water forms in the snow by melting. The actual melting temperature depends on the size of the snow particles, because the vapour pressure over the ice surface is inversely proportional to its radius. So for example particles with a radius of 0.1 mm melt at -0.001 ℃ and particles with a radius of 0.01 mm melt at -0.01 ℃ (McClung and Schaerer, 2006).

The amount of water in liquid phase within the snow is called the liquid water content. The liquid water content is either measured by the share of volume or by the share of mass of the liquid phase of the total. Therefore the volumetric liquid water content (LWC_{vol}) and the liquid water content by mass (LWC_{m}) are established terms in snow science (Fierz et al., 2009).

The presence of free liquid water is a necessary condition for the formation of wet snow avalanches. Increasing free liquid water is suspected to reduce the stability of the snow pack and therefore considered a major contributor for triggering wet snow avalanches (Mitterer and Schweizer, 2013). Wet snow avalanches are very difficult to forecast accurately since they mostly release spontaneously. The mechanical properties of wet snow avalanches, such as strength and density are depending on the liquid water content (Techel and Pielmeier, 2011).

To measure the liquid water content in the snow, a wide range of different methods is available, such as cold calorimetry, alcohol calorimetry, dilution method, and centrifugal separation. These methods are very time consuming and elaborate. It is also possible to do dielectric measurements or to estimate the volumetric liquid water by a hand test, to improve the handling of the measurement and get a faster result (Mitterer, 2012).

1.3 Flowing snow

Flowing snow in an avalanche can exhibit different flow regimes that underlie many physical properties. The appearance of snow avalanches can take various forms depending on the flow behaviour. Gauer et al. (2008) and Sovilla et al. (2007) showed that an avalanche consists out of three flow regimes which mainly differ in their density and shear rates:

1. The dense flow regime is characterized by persistent contacts between the particles and their dense packing. This dense packing allows stresses to be transmitted by force chains.
2. With increasing shear rates, a more fluid like layer evolves out of the dense flow. In this fluidized regime, where the distance between the centre of the individual particles is considerable bigger than their diameter, momentum transfer takes place mostly by collisions between the particles.
3. The dilute suspension layer is characterized as the top part of an avalanche with the lowest density. The distance between the centre of the particles is far bigger than the particles' diameter and therefore the suspended regime can be described as a flow subjected to fluid forces.

A distinctive characteristic of wet snow avalanches is that no powder cloud of dilute suspended snow forms. Higher friction between the flowing snow and the basal surface results in a lower travelling speed of wet snow avalanches in comparison to dry or mixed snow avalanches on identical terrain. For a slower avalanche also the friction between the flowing snow and the ambient air is lower, which leads to weaker turbulences that are not strong enough to lift the snow particles up and suspend them in the air (McClung and Schaerer, 2006).

1.3.1 Physical properties of flowing snow

The evolution of avalanche dynamic properties such as snow density, temperature, and free liquid water is subjected to the volume of snow in an avalanche, the morphology of the avalanche path, and the flow behaviour of the snow. Investigations by Naaim et al. (2013) on flowing snow showed that no significant development can be observed for the inertial friction coefficient, but it was found that the static friction coefficient depends on the temperature, density, and the liquid water content. Applied simulation models are largely based on the friction coefficients, but since the knowledge about the involved physics is scarce and real scale rheological measurements are hardly available, empirical calibration is the only practicable way.

Density of flowing snow

Different types of avalanches exhibit different values of densities. For example typical flow densities of powder snow avalanches have the lowest density ($\approx 10\,\mathrm{kg\,m^{-3}}$), while dry loose snow avalanches have higher densities ($100-200\,\mathrm{kg\,m^{-3}}$), which are still below the densities of wet snow avalanches ($150-300\,\mathrm{kg\,m^{-3}}$) according to McClung and Schaerer (1985). Sovilla and Bartelt (2002) found that the distribution of the snow mass in the avalanche, both horizontally and vertically, is strongly depending on basal friction and is considered to influence the dynamics of the flow. The static friction coefficient shows a linear increase for densities $>200\,\mathrm{kg\,m^{-3}}$ (Naaim et al., 2013). Higher basal friction results in an increased transport of snow from the front and the body to the tail of an avalanche and therefore changes the distribution of mass in an avalanche (Sovilla and Bartelt, 2002).

Temperature of flowing snow

Snow temperature is often neglected in up-to-date avalanche models, though its effects like altered stress, hardness, and liquid water content of the snow, modify the dynamic flow behaviour considerably. For example the onset of granulation and consequently the granule size distribution are assumed to depend on the thermal energy in the avalanche. An established method to include the effect of the temperature of the flowing snow into a model is by adjusting the friction parameters (Steinkogler et al., 2014; Vera Valero et al., 2012).

The exact evolution of the temperature of an avalanche along its path is very complicated, since entrainment of snow does not only add mass to the flow, but also supplies thermal energy (Steinkogler et al., 2014).

Vera Valero et al. (2012) found two irreversible thermodynamic processes in an avalanche flow. First the temperature balance is influenced by shear work in dependence on the mean kinetic energy, and second thermal energy is accumulated due to collision of granules. Vera Valero et al. (2012) state that the temperature of the avalanche is primarily determined by the thermal energy of the entrained snow, and that heating due to friction only played a minor role.

Liquid water content of snow

The basic requirement for wet snow is free liquid water. Wet snow avalanches can only occur when the snow temperature reaches the melting point either in the release zone or along the avalanche path (Baggi and Schweizer, 2009).

At very low liquid water contents with a volumetric percentage $< 3\,\%$ the snow crystals form well bonded ice clusters and air can still interchange continuously through the pores. The strength of the snow with bonded clusters is equal or even increases with the formation of free liquid water. For an increased volumetric liquid water content $> 8\,\%$ the bonds between crystals dissolve, and in combination with additional free liquid water strength decreases drastically (Colbeck, 1987).

Various studies on the shear strength of snow found that the strength is nearly equal for a volumetric liquid water content $\leq 6\,\%$, and decreases rapidly for higher values (Brun and Rey, 1987). Other authors state that a decrease in the snow hardness can even be observed at liquid water contents $\leq 3\,\%$ (Techel and Pielmeier, 2011).

On the one hand a serious change in strength or hardness could initiate an avalanche, and on the other hand it could have a huge influence on the flow behaviour. Naaim et al. (2013) found that low liquid water contents $< 3-4\,\%$ do not influence the flow behaviour significantly. For higher amounts of free liquid water, the static friction coefficient decreases.

Further a relation between the onset of granulation, the size distribution of the granules, and the liquid water content was assumed by Steinkogler et al. (2014).

Despite the fact that the interdependency of free liquid water and snow is topic of recent research this phenomenon is poorly understood. Further investigation based on simulations, experiments in the field, and measurements in the laboratory is inevitable to gain profound knowledge of wet snow avalanches (Mitterer, 2012).

Granulation

The grain size distribution plays a considerable role in granular flows. It is an expression of the flow properties and allows to draw conclusions about the mean velocity and the shear rate in an avalanche (Bartelt and McArdell, 2009). The variation of the particle size is the result of an interplay between aggregation and fragmentation. Snow particles are cohesive and can stick together and enlarge after collisions, but since snow is only deformable to a certain extent, the relative brittle granules can also break apart in collisions and get smaller (Steinkogler et al., 2014).

To gain knowledge about the relation between particle size distribution and flow dynamic properties, investigations on avalanche deposits have been conducted. Recent research concentrated on two important effects. First, the interdependency of granule size and internal shear rates in an avalanche, and second, the transformation of energy during collisions. Both processes have a crucial influence on granular avalanche dynamics (Bartelt and McArdell, 2009).

The simplest way to investigate the grain size distribution is to survey the deposition of real scale avalanches. Therefore a surface grain size sampling method was applied (Bartelt and McArdell, 2009; De Biagi et al., 2012). The authors measured the dimensions of granules in the deposition of avalanches manually and grouped them into size classes to generate a grading curve, similar to those established in geology. Other methods such as sieving and bulk sampling seem to be a good alternative at the first look, but turn out to be destructive and alter the size of the investigated granules.

Kobayashi et al. (2000) recreated the granulation process in a model experiment with a polyethylene bucket. They investigated the size distribution, the total number of granules that formed out of an initial volume of snow, and the hardness of those granules. The results of Kobayashi et al. (2000) indicate that the mean granule size is much smaller in dry snow avalanches than in wet snow avalanches. This is in accordance with observations of Bartelt and McArdell (2009) who further demonstrate that the grading curves tend to a log-normal distribution. In comparison, wet snow avalanches have a significantly broader grading curve than dry ones, which, according to Bartelt and McArdell (2009), is based on the reduced velocities and vertical shear gradients.

Altogether studying the granules helps to understand the flow properties that result in those observed particles, and leads to a more profound knowledge of avalanche dynamics.

Dielectric permittivity of snow

The dielectric permittivity allows to calculate the amount of free liquid water in snow. The resistance of a material in an electromagnetic field is measured by the dielectric permittivity ε. The material with the lowest resistance in an electromagnetic field is vacuum, therefore also its permittivity ε_0 is the lowest possible and called the dielectric constant. To characterize other materials, their absolute permittivity is referred to the one of vacuum and the fraction is called the relative dielectric permittivity ε_{r}.

$$\varepsilon_{\mathrm{r}} = \frac{\varepsilon}{\varepsilon_0} \tag{1.1}$$

ε_{r} = relative permittivity [ ]
ε = permittivity [ ]
ε_0 = dielectric constant [ ]

For other materials than vacuum, the dielectric permittivity is depending on the frequency of the electromagnetic field. This is described as a complex function of the frequency ν with a real part ε' and an imaginary part ε''.

$$\varepsilon(\nu) = \varepsilon'(\nu) + i\varepsilon''(\nu) \tag{1.2}$$

ε = dielectric permittivity [ ]
ν = frequency [Hz]
ε' = real part that relates to the energy stored in the material [ ]
ε'' = imaginary part that relates to the loss of energy in the material [ ]

The permittivity of snow can be considered frequency-independent in a range between 10 MHz and 1 GHz (Denoth et al., 1984). In this range the permittivity is affected neither by the grain size and shape of the ice crystals, nor by losses in the material ($\varepsilon'' \ll \varepsilon'$). It only depends on the density and the wetness of the snow.

The relative permittivities of air ($\varepsilon'_{\mathrm{air}} = 1$), ice ($\varepsilon'_{\mathrm{ice}} = 3.19$), and water ($\varepsilon'_{\mathrm{water}} = 86$) at 0 ℃ for frequencies between 1 MHz and 1 GHz are very diverse. Furthermore the following relation between the dielectric permittivity, the snow density ($100 < \rho < 500\,\mathrm{kg\,m^{-3}}$), and the volumetric liquid water content ($LWC_{\mathrm{vol}} \lesssim 8\,\%$) was found by Ambach and Denoth (1975):

$$\varepsilon' \propto \rho + {LWC_{\mathrm{vol}}}^2 \tag{1.3}$$

ε' = real part of the dielectric permittivity [ ]
ρ = density of the snow [$\mathrm{kg\,m^{-3}}$]
LWC_{vol} = volumetric liquid water content [%]

Based on these physical relations, the dielectric permittivity enables to draw conclusions about the liquid water content of snow (Denoth, 1989, 1994; Frolov and Ya. Macheret, 1999).

In sum, a pair of measurements of the real part of the dielectric permittivity and the density of a snow sample allows to calculate the liquid water content (see Section 2.3).

1.3.2 Experiments with flowing snow

For the understanding of the constitutive behaviour of flowing snow, different approaches were pursued to find a description that reflects observations in a physically correct way. One example for such a contribution are the recent experiments to investigate the rheology of snow in a large chute by Kern et al. (2004), who present their results for velocity profiles and basal shear forces from experiments with snow on a 34 m long, 2.5 m wide, and 34 ° inclined chute. Rubber bars were installed on the sliding surface to induce a basal shear layer in the downstream flow. Kern et al. (2004) showed that the measured velocity profiles exhibited a sheared basal layer and a much less sheared overlying layer. This overlying layer was approximately seven times the thickness of the basal layer and the transition between those two layers was indistinct. For a comprehensive investigation of the flow behaviour of snow with the chute two challenges have to be faced. On the one hand a multiplicity of experiments has to be conducted, and on the other hand the snow samples must resemble to each other in their physical properties (Kern et al., 2004).

Another interesting approach to investigate the flow behaviour of snow was pursued by Steinkogler et al. (2015). The aim of their work was to observe the evolution of flowing snow with special attention drawn to the granulation phenomena that occurs in snow avalanches in the field. A concrete tumbler was employed and properties of the snow samples like temperature and water content were varied. In addition, discrete element simulation of the samples in the drum was performed. The results indicated that temperature could be regarded as the substantial condition for granulation, particularly if it rose above -1 ℃. To characterize the granules, they were distinguished by their wetness according to Fierz et al. (2009) and their persistence in collisions. Based on these characteristics the granules were categorized into three granulation classes – non persistent, persistent-moist, and persistent-wet. Further research on the temperature-dependent granule size distribution as well as on the interaction between processes of different scale in an avalanche (e.g. sintering, granule interaction, and flow dynamics) is necessary to improve the understanding of avalanche dynamics (Steinkogler et al., 2015).

2 Methods

The flow behaviour of snow was investigated in a vertically rotating drum that allowed to measure a variety of physical parameters. The following chapter gives detailed information on the harvest of snow in the field, the geometry and instrumentation of the rotating drum, and the data analysis.

2.1 Harvest of snow

For the each experiment approximately 100 l of snow were used. To have a stock large enough for at least ten experiments it was necessary to go out into the field and gather new snow. The harvest was done during a cold period in the Winter 2017.

First, on January 9^{th} 2017, heavy snowfalls in the preceding days allowed to harvest approximately 1000 l of new snow in Maria Anzbach, located in Lower Austria close to Vienna. Second, due to snowfalls over night in Vienna, it was possible to gather additional 600 l of freshly fallen snow near the BOKU University of Life Sciences and Natural Resources in the 19^{th} district of Vienna, on February 1^{st} 2017. Table 2.1 displays the values of the environmental parameters of the harvest of snow on both dates.

Table 2.1: Harvest of snow: environmental parameters at the locations of the snow gathering. T_{air} is the ambient air temperature, T_{snow} is the snow temperature, and ρ is the density of the freshly fallen snow in the field.

date	location	T_{air} [°C]	T_{snow} [°C]	ρ [kg m^{-3}]
09.01.2017	Maria Anzbach	-1.0	-1.0	120
01.02.2017	Vienna	-1.5	-2.0	120

In the field, the snow was sieved with a sieve of 2 mm mesh size into boxes with a volume of 90 l. Then the boxes were shaken to force the snow to settle and increase its density. When the snow was about half its initial volume, the boxes were filled up with sieved snow and shaken again. This increased the density of the new fallen snow from original 120 kg m^{-3} to more than 250 kg m^{-3}.

The prevailing air temperatures ($T_{air} \leq -1\,℃$) allowed to transport the boxes with a pick-up truck to the cold laboratory, where they were stored at $-17\,℃$, until the snow was used for the experiments.

2.2 Rotating drum

For the experiments a vertically rotating drum was employed (see Fig. 2.1). The following section gives a description of the geometry and the instrumentation of the vertically rotating drum (Kaitna et al., 2007).

2.2.1 Geometry

The drum had a diameter of 2.45 m and a rectangular channel section of 0.45 m. The lateral walls of the cross section on the side of the drive shaft were made of steel, and on the opposite side of acrylic glass to make the flow of material observable during the experiment. To increase basal roughness a polyvinyl chloride mesh was applied to the flume bottom, and in addition semicircular risers made of wood with a height of 1 cm were installed every 20 cm along the bed to avoid basal slip. Horizontally at the right side a wiper was installed to clean the bottom surface.

To process and display the measurements, a coordinate system is assigned to the drum where the angle φ is measured from the vertical, so 0° is equivalent to the six o′clock and 90° to three o′clock position

2.2.2 The measuring system

The measuring system installed at the rotating drum consisted of two laser range finders measuring the flow height, two single point load cells, thermocouples, a torque flange, and a static photo electric sensor measuring the rotational speed. The output signals were transmitted over a telemetry to a multi channel receiver and a measurement amplifier. The amplifier was connected via Ethernet cable to a computer, where the data were recorded with the evaluation program CatManEasy.
Data from the measuring system was provided with a rate of 400 Hz.

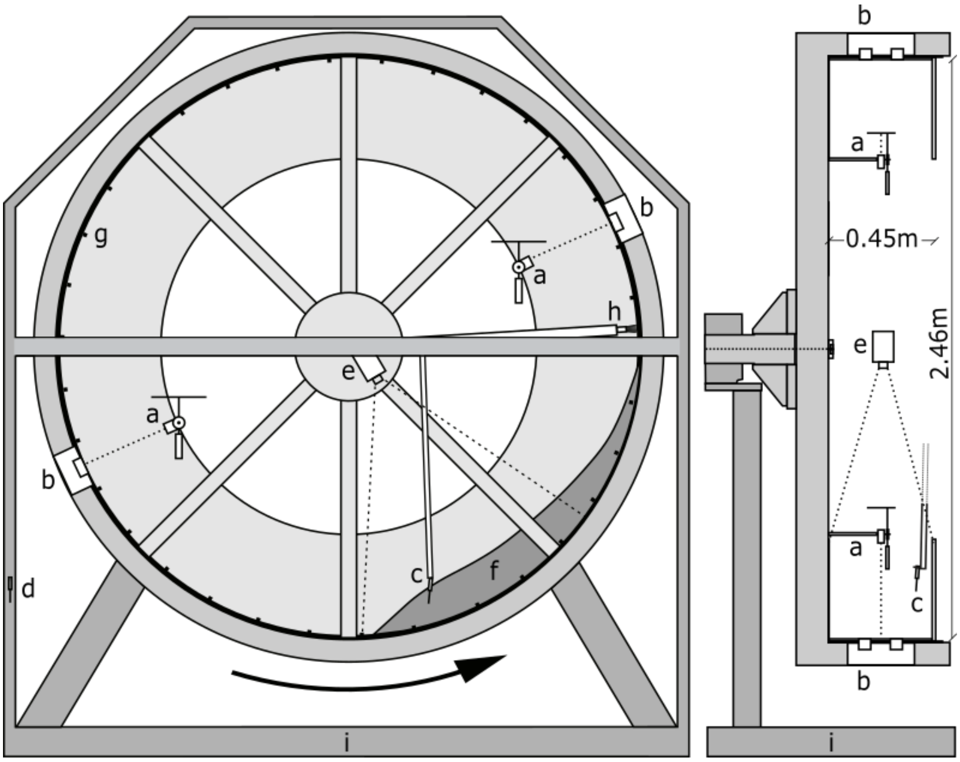

Figure 2.1: The rotating drum (adapted from Kaitna et al. (2007)): a) laser sensors for measuring flow height, b) normal and shear stress sensors, c) thermocouple in the flow, d) thermocouple in ambient air, e) camera, f) material flow, g) polyvinyl chloride mesh (height = 2 mm) and semi-circular risers (height = 10 mm every 0.2 m along the bed), h) wiper, i) steel frame

2.2.3 Measuring the normal pressure

Normal stress was measured in radial direction with two individual single point load cells. They were installed in the middle third of the channel section, displaced by 180° around the circumference. Hence two measurements of the normal stress per revolution could be recorded. The diameter of the cells was 60 mm and the accuracy was 0.1% with a maximum loading capacity of 7.2 kg.

2.2.4 Measuring the longitudinal flow profile

The longitudinal section of the flow height was measured with two laser range finders ($\lambda = 600$ nm). They were installed over the load cells in the rotating flume, measuring the flow height above the load plates.

2.2.5 Measuring the torque

The uni-axially mounted drum was connected to a motor by a torque flange. While driving the rotating drum at up to 32 rpm, the expended torque was measured at the flange continuously. The rotational speed was measured by a sliced ring and a photo electric sensor.

2.2.6 Measuring the snow temperature

Measuring the temperature of the snow in the flume was accomplished by a K-thermocouple. This thermocouple was built by a pair of wires made of different materials (NiCr and Ni) and measured the temperature based on the thermoelectric effect. To ensure measuring the temperature inside the material flow without disturbing the lobe, the thermocouple was attached to the tip of a flexible mounted threaded rod, pointing 3-5 cm over the bottom of the flume. The measurements with the thermocouple have an accuracy of 0.1 °C.

2.2.7 Camera

To relate the data provided by the sensors to visual pictures of the experiment a video camera was used. It was mounted in the middle of the drum on a tripod, facing the flume bottom perpendicular and aligned to capture the front of the flow. The resolution was 640 x 480 and 1920 x 1080 respectively, and the frame rate was 30 pictures per second.

Videos were recorded at the start, middle and end of every experiment, and it was attempted to catch some pictures of significant changes in the flow behaviour throughout the experiments.

2.3 Moisture sensor for the liquid water content

Denoth (1994) developed a portable device to measure the dielectric permittivity of snow. It takes measurements with a frequency of 20 MHz and is optimized for the use in the field. The measurement principle is based on a bridge circuit. This bridge transition has to be balanced first with the sensor in cool air, and second within the snow. The results of the bridge voltage for air (U_{ref}, ϵ'=1) and for snow (U) allow to calculate the dielectric permittivity:

$$\varepsilon' = 1 + k \cdot \log\left(\frac{U}{U_{\mathrm{ref}}}\right) \tag{2.1}$$

ε' = real relative permittivity of snow [ ]
k = sensor-specific calibration factor [ ]
U = bridge voltage with sensor in snow [V]
U_{ref} = bridge voltage with sensor in cool air [V]

To calculate the volumetric liquid water content, it is necessary to take accompanying measurements of the snow density for every recorded permittivity. The amount of liquid water per volume can be calculated according to:

$$LWC_{\mathrm{vol}} = 4.96 \cdot \left[k \cdot \log\left(\frac{U}{U_{\mathrm{ref}}}\right) - 2 \cdot \rho_{\mathrm{rel}}\right] \tag{2.2}$$

LWC_{vol} = volumetric liquid water content [%]
k = sensor-specific calibration factor [ ]
U = bridge voltage with sensor in snow [V]
U_{ref} = bridge voltage with sensor in cool air [V]
ρ_{rel} = snow density relative to the density of water [ ]

If the dielectric permittivity is measured by a device directly without the necessity to balance a bridge circuit manually, Equation 2.2 simplifies to:

$$LWC_{\mathrm{vol}} = 4.96 \cdot [\varepsilon' - 1 - 2 \cdot \rho_{\mathrm{rel}}] \tag{2.3}$$

LWC_{vol} = volumetric liquid water content [%]
ε' = real relative permittivity of snow [ ]
ρ_{rel} = snow density relative to the density of water [ ]

In the experiments with the rotating drum a moisture sensor (Decagon 5TM) was used. This sensor was originally designed to measure the moisture and temperature of soil and was capable of directly measuring the dielectric permittivity, so Equation 2.3 could be applied.

The sensor consisted out of a Polyurethane coated body with three prongs. The temperature was determined by a thermistor which is coupled to the prongs. A 70 MHz oscillating electromagnetic field was provided to the prongs and depending on the surrounding material, a certain electric charge was stored in them. The microprocessor in the sensor's body then related the amount of stored charge in the prongs to a value of dielectric permittivity ε.

Since it was not possible to measure the moisture directly, the volumetric liquid water content was correlated to the dielectric permittivity and the density of the material via a transfer equation. The resolution of the dielectric permittivity was 0.1 for ε from 1 to 20, and 0.75 for ε from 20 to 80 with an accuracy of ± 1 for ε from 1 to 40, and $\pm 15\,\%$ for ε from 40 to 80. The relation between liquid water content and dielectric permittivity is different for every material, so the sensor needs to be calibrated for every individual material.

2.4 Manual measurements of the density and the liquid water content

The dielectric permittivity and the density of the flow material were measured manually every 300 s. A sample was extracted out of the flume with a bailer of known mass and volume. The exactly filled bailer was weight and the Decagon 5TM sensor was introduced into the material. It has to be mentioned that with densities over approximately 500 $\mathrm{kg\,m^{-3}}$ it was getting difficult to insert the sensor into the snow without damaging it. Further for the experiments 170215_09 to 170216_13 it was not possible to fill the bailer without air entrapped between the granules. Therefore cubic samples with 5 cm side length were cut out of the granules and weight to measure the density.

The Decagon 5TM sensor also measures the investigated material's temperature. Since the thermistor is located in the polyurethane overmoulding and it was difficult to insert the sensor fully into very dense snow, the temperature measurement sometimes read high (due to elevated environmental air temperature). Further it took the sensor up to 2 minutes to adapt to snow temperatures.

2.5 Experiments

For the investigation of the flow behaviour of snow in the rotating drum it was necessary to identify the present boundary conditions and to develop a procedure to execute the experiments.

2.5.1 Relevant experimental parameters

One very important parameter that could technically easy be adjusted at will, is the rotational speed. Therefore it can be regarded a controlled boundary condition. Different rotational speeds lead to different results for the physical properties of the flowing snow.

A second basic condition is the ambient air temperature. It has an influence on the investigated material, since for example at higher temperatures there is more thermal energy available to warm the snow. Due to the fact that the rotating drum was located in an outdoor facility the air temperature could not be altered, but the time to conduct the experiments could be chosen. That makes the air temperature a relatively controlled boundary condition.

2.5.2 Execution of the experiments

The experiments were carried out in an outdoor facility. They were started by getting a box of snow ($\approx 100\,\mathrm{l}$) from the cold lab and sieving it with a 2 mm mesh sized sieve. On the one hand this broke bonds that formed by sintering within the material while stored, and on the other hand increased the density to approximately $250\,\mathrm{kg\,m^{-3}}$.

Then the snow was filled into the rotating drum, turning special attention to the load cells and laser sensors being unaffected by the material. Afterwards the measurement system was started and the rotational speed increased until the pre-set velocity.

The first pre-set speed was 5.3 rpm because this was the lowest velocity where steady flow regime could be obtained in the experiments. Second speed was 15 rpm due to the fact that is was the fastest speed allowing the manual measurements to be executed. Especially the extraction of material with the bailer was not feasible at higher speeds, because the rotating mounting devices of the two laser sensors only left an interval of less than 2 s for sampling.

The time span of the experiments was chosen until the temperature of the snow was mostly constant and the morphology of the flowing lobe did not change its structure any more, or the majority of the snow was melted so that proceeding the experiment was of no further scientific interest. For some experiments the data communication froze and the experiments had to be terminated.

2.6 Data evaluation

The measurements were provided in the program CatManEasy. For further analysis ASCII data files were exported to MATLAB.
The name of the files was chosen corresponding to the name of the experiments: YYMMDD_##. "YY" refers to the year, "MM" to the month, "DD" to the day and "##" to the consecutive number of the experiments (e.g. 170123_01).

2.6.1 Analysis of the normal stress measurements

For the analysis of the basal normal stress of the flowing snow, the measurements had to be evaluated. Due to the rotation of the drum and the self weight of the force plates a sine-wave form was observed in the signal of the normal stress. This means if the drum was employed without any flowing material, a sinusoidal signal with the same frequency as the rotational speed was generated. When the flow of a material was investigated in the drum, the normal stress of the flow added to the sine-wave form. To get reasonable results for the normal stress of the flowing material, this sinusoidal signal had to be subtracted from the measuring signal. This was done by a MATLAB-script, originally designed by Prenner (2011).

2.6.2 Calculation of the density

The bulk density of the flow was calculated from the measurements of the flow height and the normal pressure according to Equation 2.4. The laser range finders measured the height of the snow thrown back by the wiper at the tail of the flow. To eliminate this misrepresentation of the flow height the density was calculated in an interval from 0° to 60°.

$$\rho_{\text{calc}} = \frac{p}{g \cdot h} \tag{2.4}$$

ρ_{calc} = calculated density [$\mathrm{kg\,m^{-3}}$]
p = normal pressure [Pa]
g = gravitational acceleration [$\mathrm{m\,s^{-2}}$]
h = flow height [m]

2.6.3 Calculation of the total variation of the normal pressure

The total variation was used as an indicator to estimate the point of time for the onset of granulation. If the flow consisted out of loose snow, the variation of the normal pressure measurements was very low compared to the variation after granulation occurred. To identify the moment when granules started to form and hence the variation of the measured signal started to rise, the total variation was calculated in an interval from 0° to 45° according to Equation 2.5. The upper limit was chosen because the calculation produced more meaningful results for this interval than for the entire length of the flow.

$$V_{\text{total}} = \int_0^{45} \left| \frac{\partial p}{\partial \varphi} \right| \, \mathrm{d}\varphi \tag{2.5}$$

V_{total} = total variation of the normal pressure [Pa/ °]
p = normal pressure [Pa]
φ = angle [°]

2.6.4 Calculation of the deviation angle θ_{COG}

The deviation angle of the flow profile's centroid was calculated from the laser measurements. The centre of the area under the flow profile was ascertained in a range between 0° and 60°. It was necessary to use this range of angle in order to cut off the tail of the measurements, where snow thrown back by the wiper and the wiper itself were registered by the laser sensor. The vertical deviation angle of the centroid of the flow could then be computed for every revolution of the drum (see Figure 2.2).

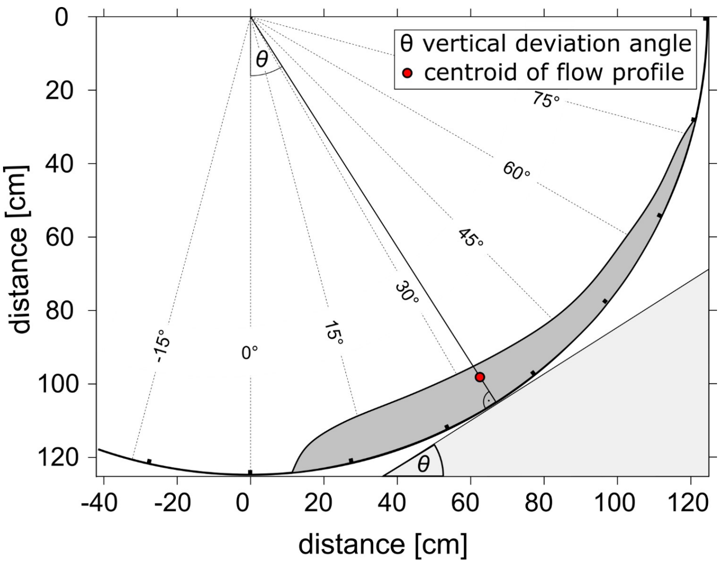

Figure 2.2: The centroid of the flow profile and the according vertical deviation angle θ_{COG}.

2.6.5 Calculation of the travel distance

The travel distance of the flowing material throughout the experiment was calculated according to Equation 2.6:

$$d = \frac{f_{\mathrm{rot}}}{60} \cdot t \cdot r^2 \cdot \pi \tag{2.6}$$

d = travel distance of the material [m]
f_{rot} = rotational speed [rpm]
t = time [s]
r = radius of the drum [m]

3 Results

A total of 13 experiments were conducted in a range of temperature between − 5 °C and + 10 °C. Seven experiments were conducted with a rotational speed of approximately 15 rpm and six with 5.3 rpm. A list of all the experiments, their rotational speed, and their according air temperature is displayed in Table 3.1.

Table 3.1: Overview of conducted experiments: number of the experiment, date, rotational speed, and ambient air temperature

experiment no.	date	f_{rot} [rpm]	T_{air} [°C]
170123_01	23.01.2017	15.0	− 4.6
170123_02	23.01.2017	15.0	− 4.8
170124_03	24.01.2017	14.8	− 4.6
170124_04	24.01.2017	5.3	− 4.1
170124_05	24.01.2017	5.3	− 4.0
170125_06	25.01.2017	5.3	− 0.8
170125_07	25.01.2017	15.0	0.0
170215_08	15.02.2017	15.2	+ 6.9
170215_09	15.02.2017	15.2	+ 7.9
170215_10	15.02.2017	15.2	+ 9.2
170216_11	16.02.2017	5.3	+ 3.2
170216_12	16.02.2017	5.3	+ 4.7
170216_13	16.02.2017	5.2	+ 4.8

Depending on the rotational speed and ambient air temperature, different developments and results for the measured parameters were observed. The following sections give an overview over the evolution of the measured and calculated parameters, such as temperature of the flowing material, density, and volumetric liquid water content throughout the experiments. Moreover experiments are compared to each other, to point out similarities and interesting differences between them.

3.1 "Cold" experiments below air temperatures of −4 ℃

Five experiments were conducted at ambient air temperatures below −4 ℃. Three of them (170123_01, 170123_02 & 170123_03) with a rotational speed of approximately 15 rpm and two of them (170124_04 & 170124_05) with 5.3 rpm.

3.1.1 Evolution of the snow temperature

In Figure 3.1 two representative graphics for the temperature of the snow and ambient air plotted over the duration of a slow (5.3 rpm) and a fast (15 rpm) experiment are displayed.

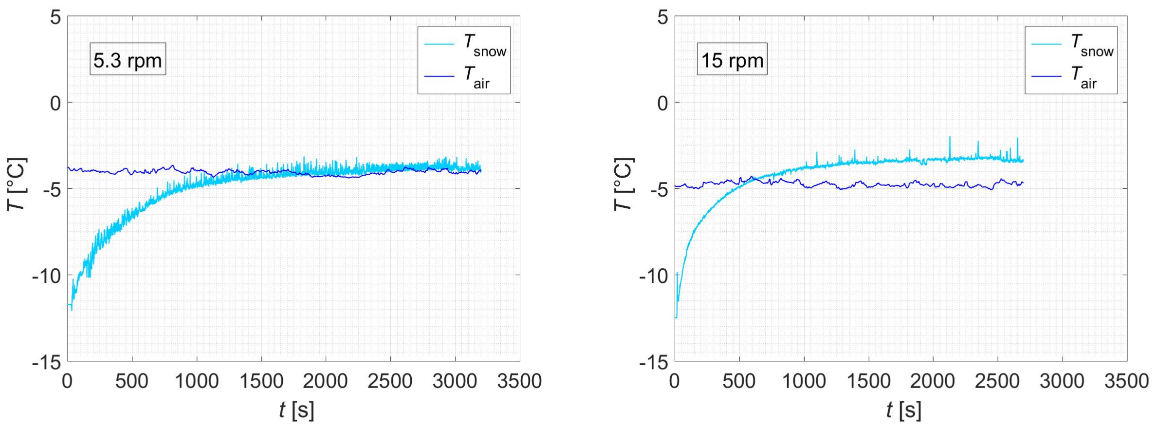

Figure 3.1: Temperature of flowing snow and ambient air, each for a representative experiment with 5.3 rpm (170124_04, left) and 15 rpm (170123_02, right).

For the experiments with a rotational speed of approximately 15 rpm the evaluation showed that the temperature of the snow increased significantly over the ambient air temperature. In contrast, for the experiments with only 5.3 rpm, the temperature of the flowing lobe only increased very slightly above the air temperature. For example, as displayed in the graphics in Figure 3.1, the difference between the temperature of the snow and the air was more than 1 ℃ for 15 rpm, whereas it was less than 0.5 ℃ for 5.3 rpm.

3.1.2 Flow height and density

In Figure 3.2 two representative graphics for the evolution of the flow profile plotted over the duration of a fast (15 rpm) and a slow (5.3 rpm) experiment are displayed.

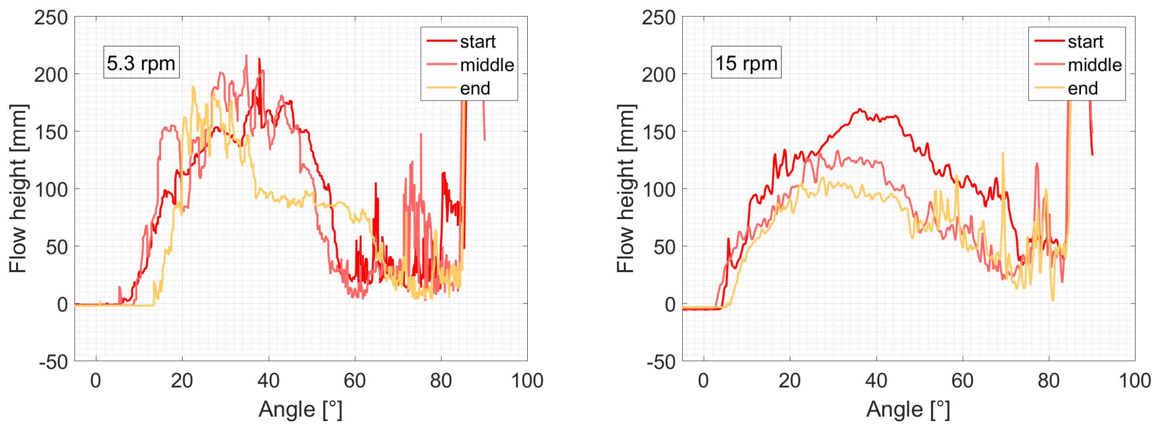

Figure 3.2: The evolution of the flow profile for a representative experiment with 5.3 rpm (170124_04, left) and 15 rpm (170123_02, right). *'Start'*, *'middle'*, and *'end'* refer to revolution *004*, *100*, and *200* for 5.3 rpm (left), and revolution *004*, *200*, and *400* for 15 rpm (right).

It was observed that the flow height decreased over the duration of all the conducted experiments at air temperatures below -4 ℃. One can see that at an angle of approximately 90°, the flow height showed very high values, because the laser sensor measured the wiper that cleaned the bottom of the cross section. The swept material was then thrown back into the flow. This could be observed in the measurements of the laser sensors at angles between approximately 60° and 89° for example in the left graphic of Figure 3.2. Further a representative series of video frames of the flowing loose snow is shown in Figure 3.3.

Figure 3.3: Frames to illustrate the steady flow behaviour. From left to right: One can observe that the front of the flowing lobe is always at the same position.

Since the mass of the flowing material was the same throughout the experiment and the flow height decreased, the density of the snow increased. Figure 3.4 shows the increase of density measured manually with the bailer and the scale as well as the density calculated according to Equation 2.4 for two experiments.

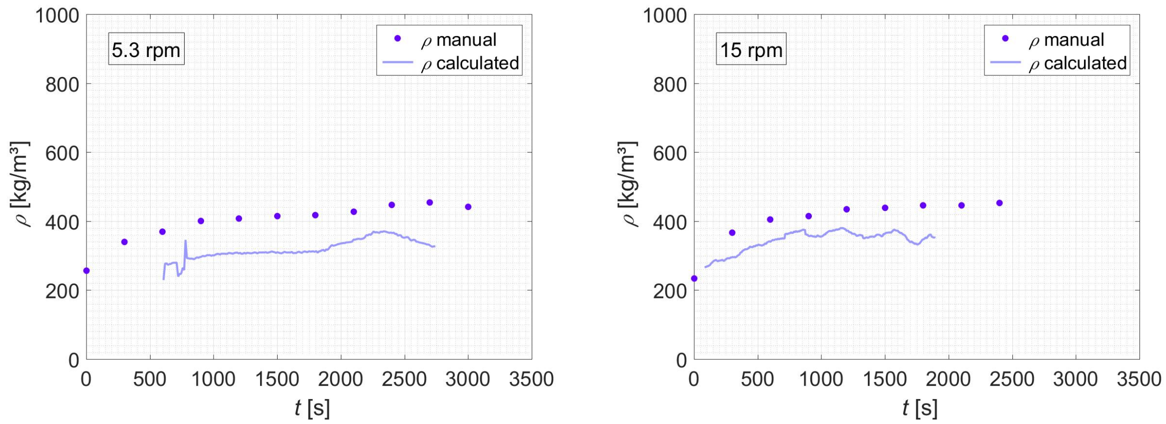

Figure 3.4: The evolution of the density measured manually and calculated out of flow height and normal pressure data for a representative experiment with 5.3 rpm (170124_04, left) and 15 rpm (170123_02, right).

3.1.3 Evolution of the volumetric liquid water content

In Figure 3.5 two representative graphics for the measurements of the volumetric liquid water content plotted over the duration of a slow (5.3 rpm) and a fast (15 rpm) experiment are displayed. The temperature of the flowing snow and ambient air are included in the graphics, to illustrate the relation between T_{snow} and the LWC_{vol}.

Water changes its phase from ice (and snow) to liquid water at 0 ℃ at an ambient pressure of 10^5 Pa. Since the temperature of the snow did not exceed -2 ℃ in any experiment conducted at air temperatures below -4 ℃, no free liquid water formed, and the volumetric liquid water content was approximately 0 % throughout the whole duration of the all those experiments, as one can observe in Figure 3.5.

3.1.4 Center of gravity

In Figure 3.6 two representative graphics for the calculated centre of gravity for each revolution plotted over the duration of a slow (5.3 rpm) and a fast (15 rpm) experiment are displayed.

The vertical deviation angle in the slow experiments was a little bit higher than in the fast experiments. An interesting phenomenon can be observed for the slow experiment in

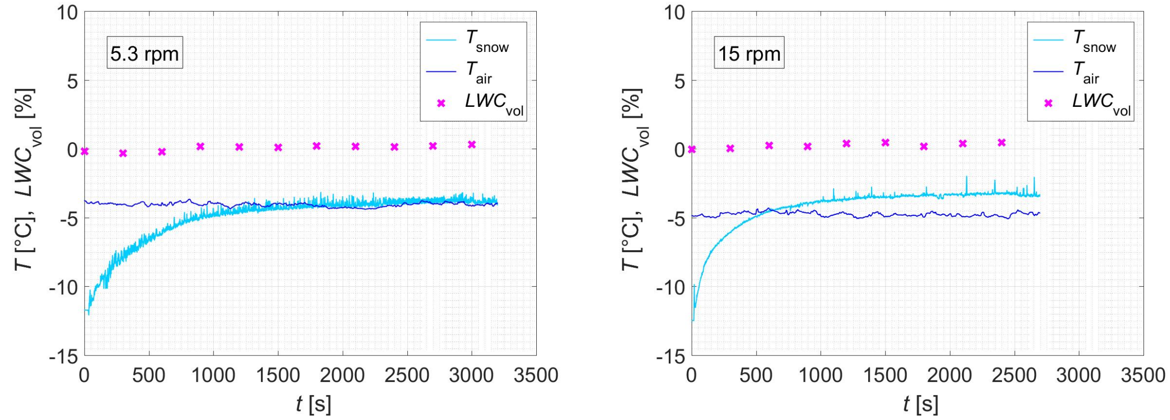

Figure 3.5: Volumetric liquid water content, temperature of flowing snow and ambient air, each for a representative experiment with 5.3 rpm (170124_04, left) and 15 rpm (170123_02, right).

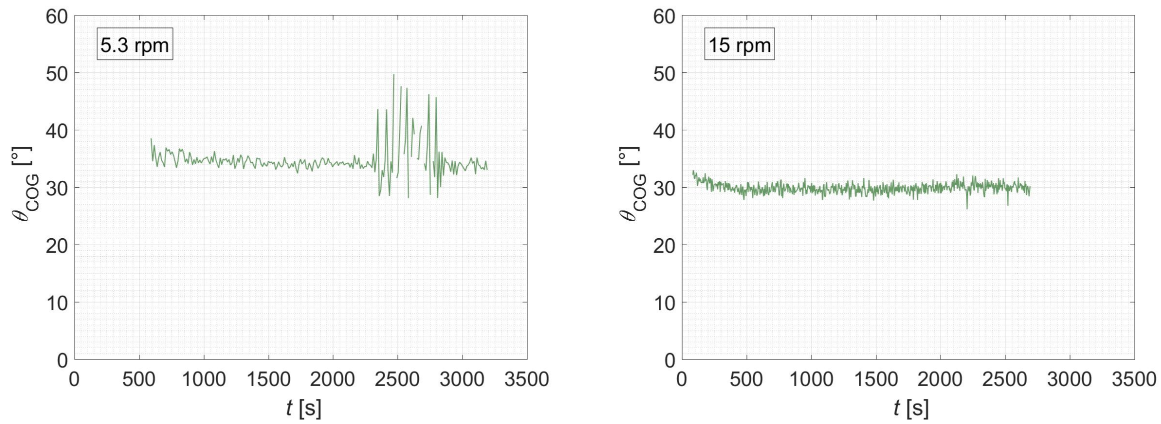

Figure 3.6: Vertical deviation angle θ_{COG} of the centre of gravity, for a representative experiment with 5.3 rpm (170124_04, left) and 15 rpm (170123_02, right).

Figure 3.6. In the range between 2300 s and 2800 s, the deviation angle deflected to very high and very low values because the flow was not steady, but stuck to the bottom, got transported upwards, and then sled down in one piece as a bulk (stick-slip behaviour). This resulted in either relatively high or very low deviation angles.

3.2 Experiments around air temperatures of 0 ℃

Two experiments have been conducted at an ambient air temperature around 0 ℃. One (170125_06) with a rotational speed of 5.3 rpm and the other (170125_07) with a rotational speed of 15 rpm.

3.2.1 Evolution of the snow temperature

In Figure 3.7 the two graphics for the temperature of the snow and ambient air plotted over the duration of a slow (5.3 rpm) and a fast (15 rpm) experiment are displayed.

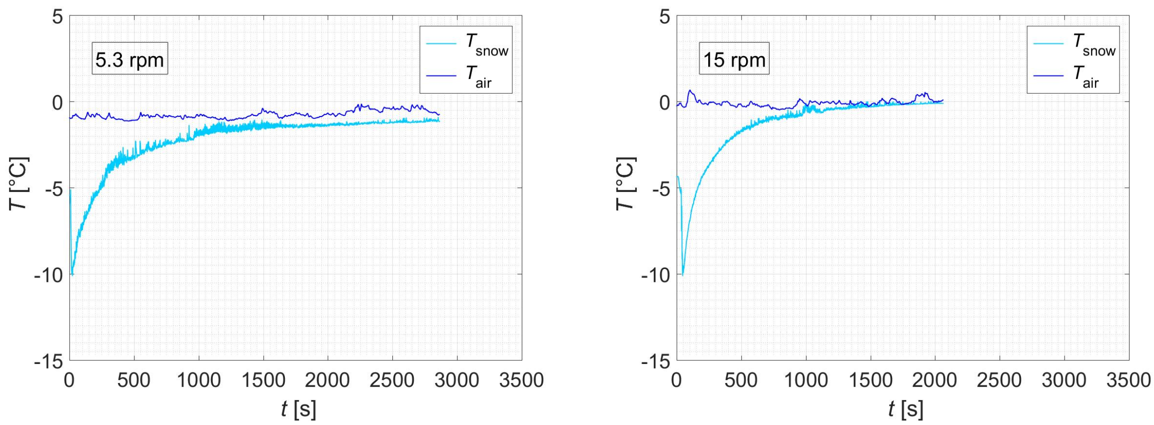

Figure 3.7: Temperature of flowing snow and ambient air, each for an experiment with 5.3 rpm (170125_06, left) and 15 rpm (170125_07, right).

For the experiment with 5.3 rpm (20170125_06) the snow increased its temperature until it nearly reached the temperature of the ambient air. At the end of the experiments, the snow temperature was still significantly below the air temperature (Fig. 3.7, left). In the experiment performed with 15 rpm (20170125_07) the results show a quicker increase of the temperature of the snow than in the experiments with 5.3 rpm. Further, the snow warmed until -0.1 ℃ and then was nearly the same temperature as the ambient air (Fig. 3.7, right).

3.2.2 Flow height and density

In Figure 3.8 two representative graphics for the evolution of the flow profile plotted over the duration of a slow (5.3 rpm) and a fast (15 rpm) experiment are displayed.

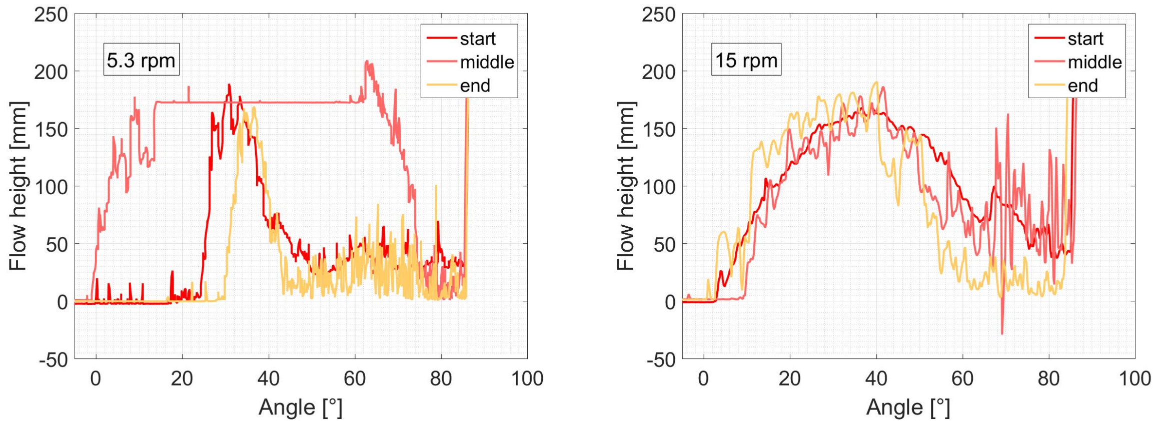

Figure 3.8: The evolution of the flow profile for a representative experiment with 5.3 rpm (170125_06, left) and 15 rpm (170125_07, right). *'Start'*, *'middle'*, and *'end'* refer to revolution *004*, *100*, and *200* for 5.3 rpm (left), and revolution *004*, *200*, and *400* for 15 rpm (right).

The graphics in Figure 3.8 point out two interesting aspects of the experiments done with the rotating drum.

First, on the left side of Figure 3.8 at the graph *'middle'*, one can see a phenomenon that appeared throughout some of the experiments, independent of ambient air temperature. The flowing material stuck to the basal sliding surface, got transported as a whole bulk in the drum without sliding on the bottom of the cross section, and when the static friction was overcome, the bulk sled down in one piece. Video frames of this effect recorded by the camera are shown in Figure 3.9.

Second, in the experiment 170125_07 granules formed around revolution 200. This could be observed in the shape of the *'middle'*- and *'end'*-graph of the flow height, on the right chart of Figure 3.8 and in the video frames of the flow in Figure 3.10.

Figure 3.11 shows the evolution of the density. The snow granules in the experiment with 15 rpm (right) had a final manually measured density of 510 kg m^{-3} whereas the calculated bulk density of the flow decreased drastically after granules formed around 955 s. In the slower experiment (left), where loose snow prevailed, the calculated density and the manually measured density had a relative small discrepancy compared to the fast experiment.

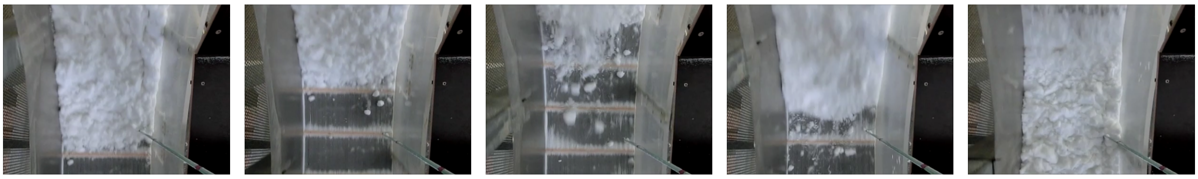

Figure 3.9: Frames to illustrate the stick-slip flow behaviour. From left to right: flowing material sticks to the basal sliding surface – gets transported as a bulk up to the wiper – when the static friction is overcome it starts to slide – the bulk slides downwards – the snow sticks to the basal surface again.

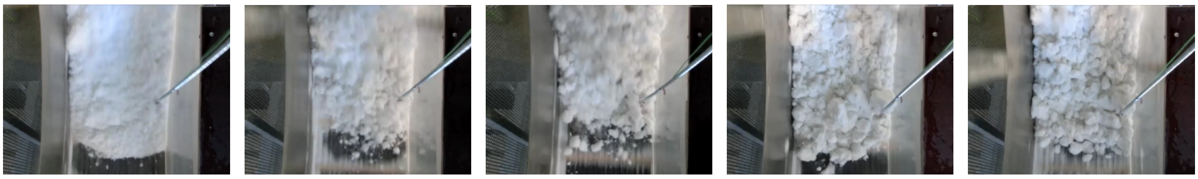

Figure 3.10: Frames to illustrate the granulation process. From left to right: loose snow – small granules start to form in the loose snow – granules become bigger while there is still loose snow – granulation process is finished – granule size increases

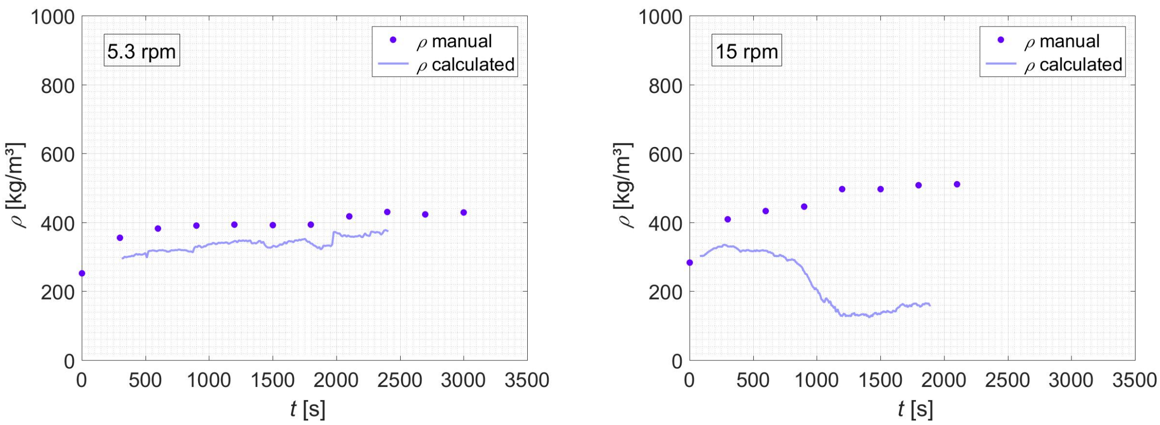

Figure 3.11: The evolution of the density measured manually and calculated out of flow height and normal pressure data for a representative experiment with 5.3 rpm (170125_06, left) and 15 rpm (170125_07, right).

3.2.3 Evolution of the volumetric liquid water content

In Figure 3.12 two representative graphics for the volumetric liquid water content plotted over the duration of a slow (5.3 rpm) and a fast (15 rpm) experiment are displayed. The temperature of the flowing snow and ambient air are included in the graphics, to illustrate the relation between T_{snow} and LWC_{Vol}.

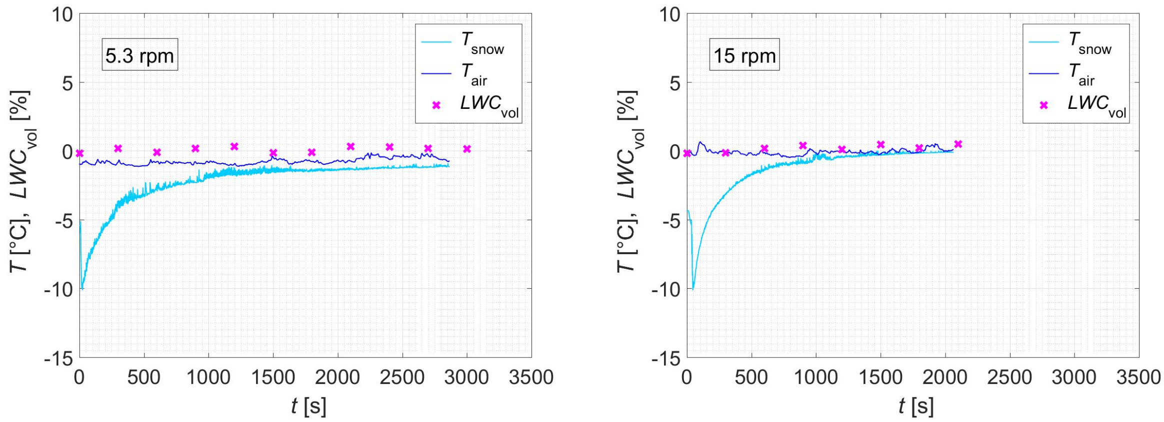

Figure 3.12: Volumetric liquid water content, temperature of flowing snow and ambient air, each for an experiment with 5.3 rpm (170125_06, left) and 15 rpm (170125_07, right).

In the two experiments around an air temperature of approximately 0 ℃ the flowing snow increased its temperature nearly up to the liquefaction point. But as Figure 3.12 (left) shows, the flowing lobe only heated up to -1 ℃ and the material did not get warm enough for a change of phase. For the fast experiment (15 rpm, Fig. 3.12 (right)) the snow increased its temperature just below the melting point. But over the duration of the experiment no free liquid water formed, because otherwise the volumetric liquid water content would have increased.

3.2.4 Total variation of the normal pressure

In Figure 3.13 two representative graphics for the total variation of the normal pressure for each revolution plotted over the duration of a slow (5.3 rpm) and a fast (15 rpm) experiment are displayed.

The graph of the slow experiment (Fig 3.13, left) showed no significant rise or trend, whereas the values in Fig 3.13 (right) started to increase at approximately 955 s. The behaviour of the two graphs was an indicator for the formation of granules. In experiment

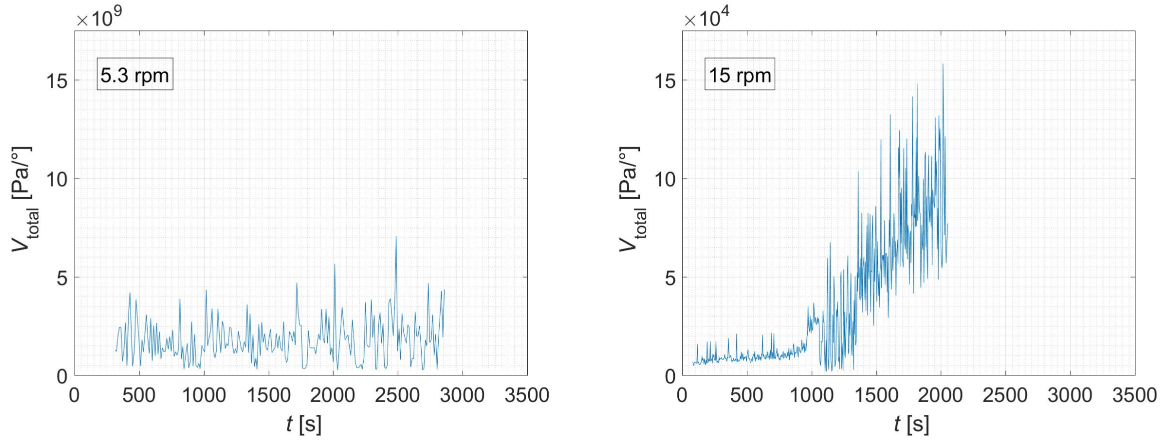

Figure 3.13: Total variation of the normal pressure, for a representative experiment with 5.3 rpm (170125_06, left) and 15 rpm (170125_07, right).

170125_06 no granules formed and therefore the total variation looks rather similar throughout the whole experiment. When granulation occurred in experiment 170125_07, the signal of the force plate changed and therefore the total variation increased.

3.2.5 Centre of gravity

In Figure 3.14 two representative graphics for the calculated centre of gravity for each revolution plotted over the duration of a slow (5.3 rpm) and a fast (15 rpm) experiment are displayed.

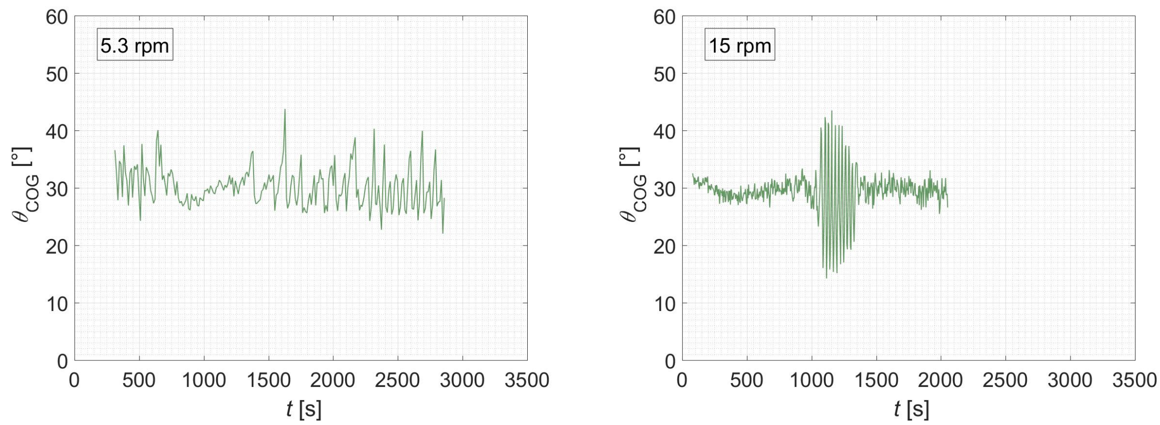

Figure 3.14: Vertical deviation angle θ_{COG} of the centre of gravity, for a representative experiment with 5.3 rpm (170125_06, left) and 15 rpm (170125_07, right).

The graph of the vertical deviation angle of the experiment 170125_06 (Fig 3.14, left)

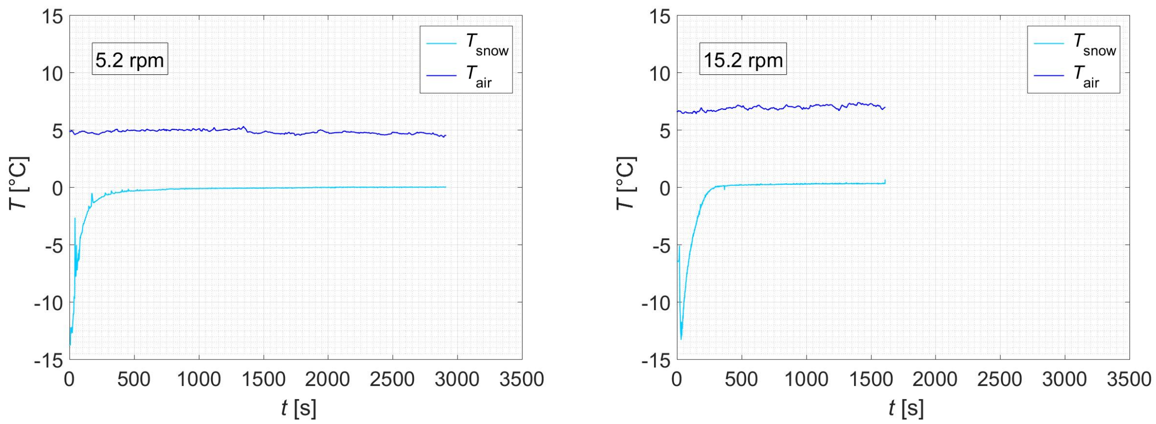

Figure 3.15: Temperature of flowing snow and ambient air, each for an experiment with 5.2 rpm (170216_13, left) and 15.2 rpm (170215_08, right) .

has a big mean variation throughout the whole experiment. The reason for this effect is the stick-slip behaviour that was observed while conducting the experiment. This is also documented by the results of the measurements of the flow height (Fig 3.8, left), where the stick-slip flow behaviour is recorded in the *'middle'*-graph. In the experiment 170125_07 (Fig 3.14, right) granules formed around revolution 200. The bulk flow then changed its flow behaviour from steady to stick-slip between 1000 s and 1500 s.

3.3 "Warm" experiments above air temperatures of + 4 °C

Five experiments have been conducted at ambient air temperatures above + 4 °C. Three of them (170215_08, 170215_09 & 170215_10) with a rotational speed of 15.2 rpm and two of them (170216_12 & 170216_13) with approximately 5.3 rpm.

3.3.1 Evolution of the snow temperature

In Figure 3.15 two representative graphics for the temperature of the snow and ambient air plotted over the duration of a slow (5.2 rpm) and a fast (15.2 rpm) experiment are displayed.

In the experiments where the air temperature was higher than + 4 °C, the temperature of the flowing snow increased very quickly to 0 °C. The difference of the rotational speed between 5.2 rpm and 15.2 rpm did not have a very relevant influence on the speed of this

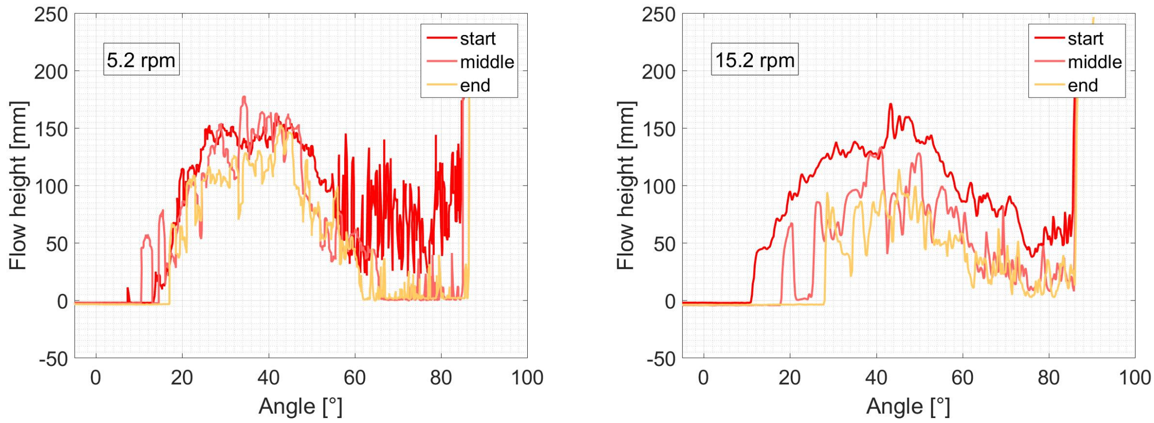

Figure 3.16: The evolution of the flow profile for a representative experiment with 5.2 rpm (170216_13, left) and 15.2 rpm (170215_08, right). *'Start'*, *'middle'*, and *'end'* refer to revolution *004*, *120*, and *200* for 5.2 rpm (left), and revolution *004*, *200*, and *392* for 15 rpm (right).

increase, as one can obtain in Figure 3.15.

3.3.2 Flow height and density

In Figure 3.16 two representative graphics for the evolution of the flow profile plotted over the duration of a slow (5.2 rpm) and a fast (15.2 rpm) experiment are displayed.

In both of the experiments after starting the drum, it took only a few revolutions until the onset of granulation occurred. For the *'start'*-graph in both experiments one can still see the profile of the flowing loose snow. Later the flow consisted out of granules in all the experiments conducted at air temperatures above + 4 °C. This is represented by the *'middle'*- and *'end'*-graph in both diagrams of Figure 3.16.

The density of the snow was measured manually every 300 s (Fig 3.17). The granules consisted out of very hard snow, which made it especially challenging to measure their density with the bailer without air inclusions. In the right plot the correlating calculated bulk density decreased immediately after the start of the experiment. And in the left plot, the calculated density has a big gap due to malfunction in the data analysis of the load cell and laser sensor data. Manual measurements show that the final density was far over 700 $\mathrm{kg\,m^{-3}}$, which is a very high value for snow.

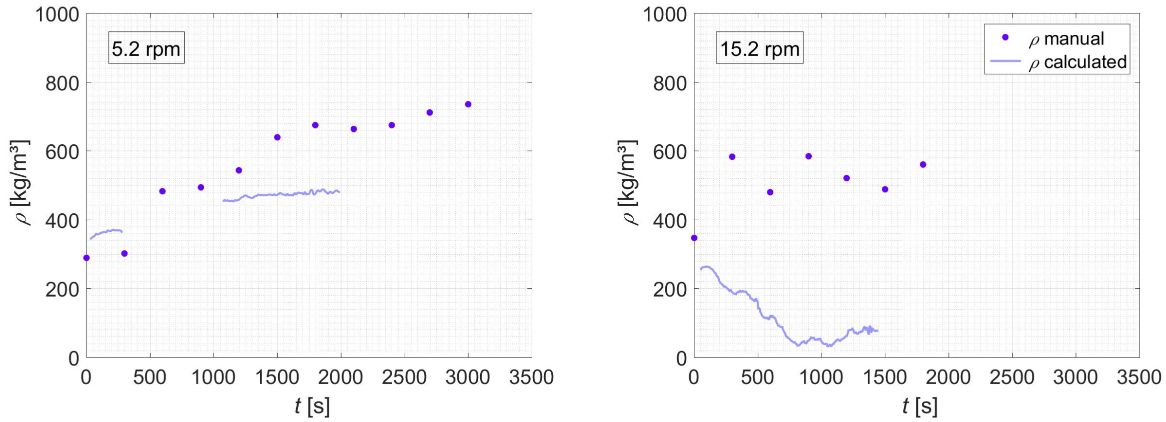

Figure 3.17: The evolution of the density measured manually and calculated out of flow height and normal pressure data for a representative experiment with 5.2 rpm (170216_13, left) and 15.2 rpm (170215_08, right).

3.3.3 Evolution of the volumetric liquid water content

In Figure 3.18 two representative graphics for the volumetric liquid water content plotted over the duration of a slow (5.2 rpm) and a fast (15.2 rpm) experiment are displayed. The temperature of the flowing snow and ambient air are included in the graphics, to illustrate the relation between T_{snow} and LWC_{Vol}.

After the temperature of the snow reached 0 °C free liquid water started to form, hence the volumetric liquid water content increased. Over the duration of the conducted experiments, the water content rose continuously up to 25 % and over. At the end of some experiments, the flowing material was dripping wet and looked like slush.

3.3.4 Total variation of the normal pressure

In Figure 3.19 two representative graphics for the total variation of the normal pressure for each revolution plotted over the duration of a slow (5.2 rpm) and a fast (15.2 rpm) experiment are displayed. The graph of the slow experiment (Fig 3.19, left) has a major gap between 750 s and 1200 s. This is due to problems with the analysis of the measured data. One can see that the total variation starts to increase just before the gap at approximately 400 s. For the fast experiment (Fig 3.19, right) the data series was complete and a distinct increase could be observed at 285 s when granules formed.

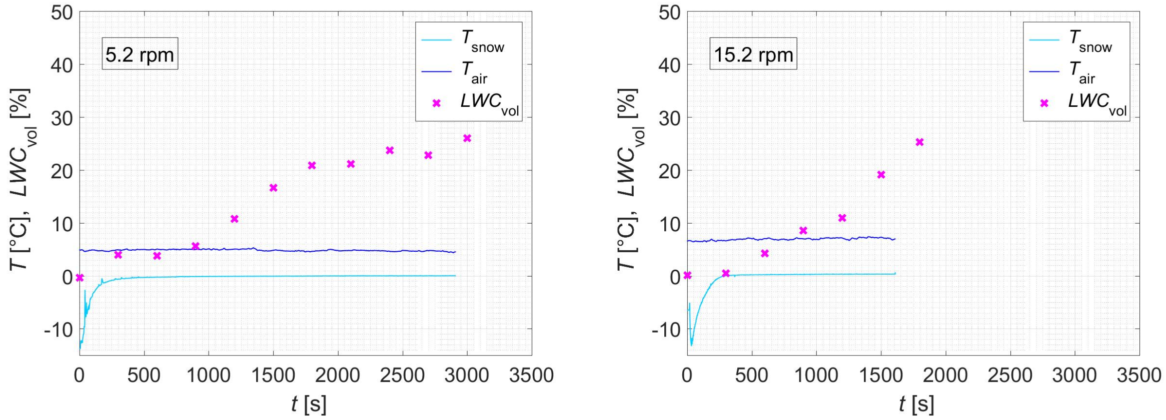

Figure 3.18: Volumetric liquid water content, temperature of flowing snow and ambient air, each for a representative experiment with 5.2 rpm (170216_13, left) and 15.2 rpm (170215_08, right).

3.3.5 Center of gravity

In Figure 3.20 two representative graphics for the calculated centre of gravity for each revolution plotted over the duration of a slow (5.2 rpm) and a fast (15.2 rpm) experiment are displayed.

The graph of the vertical deviation angle of the experiment 170216_13 (Fig 3.20, left) shows the evolution of loose snow to granules between the beginning of the experiment and approximately 700 s. Then there are a few gaps in the data, due to problems with the data analysis. In the fast experiment 170215_08 (Fig 3.20, right), the granules formed after 285 s. One can see the increase to higher vertical deviation angles until 300 s. The variation of the graph mainly resulted from big granules that were rolling from the tail over the top surface of the flow to the front sometimes. This changed the position of the flow profiles centroid significantly.

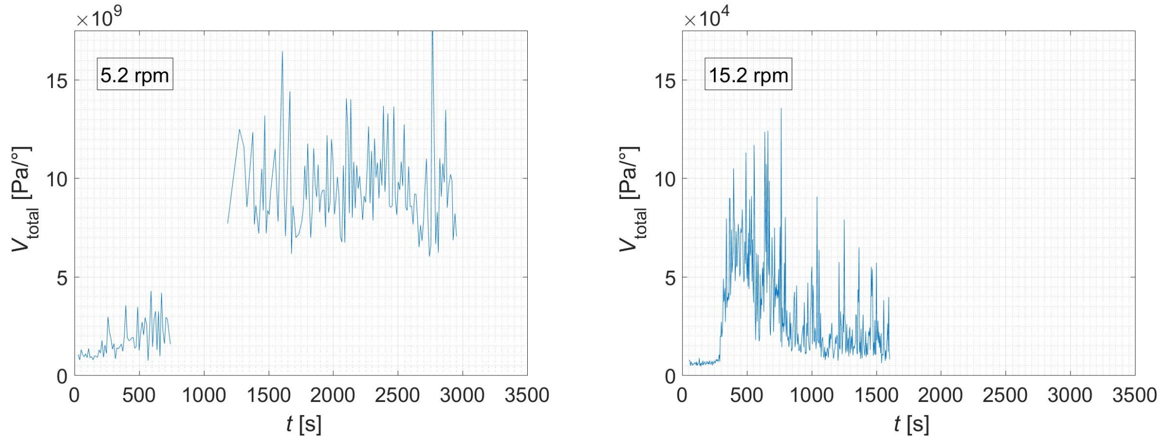

Figure 3.19: Total variation of the normal pressure, for a representative experiment with 5.2 rpm (170216_13, left) and 15.2 rpm (170215_08, right).

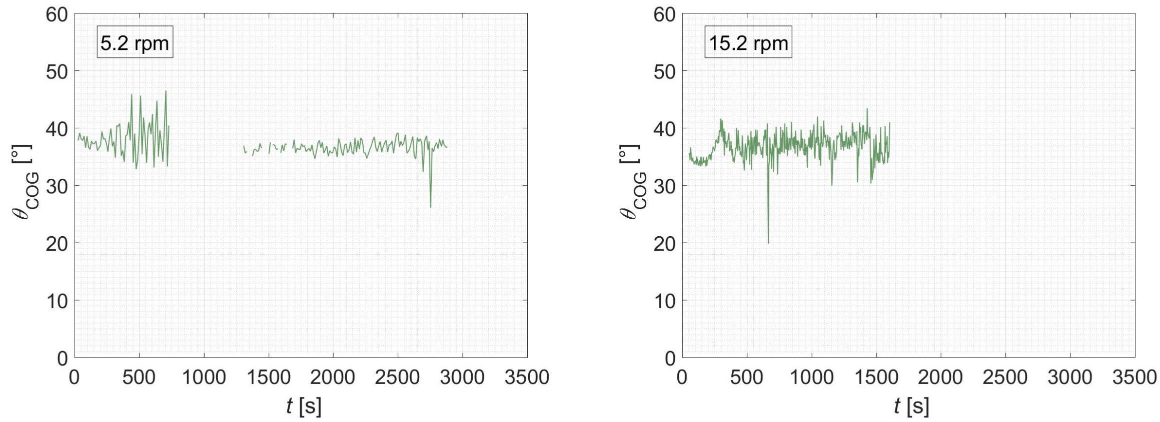

Figure 3.20: Vertical deviation angle θ_{COG} of the centre of gravity, for an experiment with 5.2 rpm (170216_13, left) and 15.2 rpm (170215_08, right).

3.4 Meta-analysis of the experiments

This section gives an overview over the evolution of the snow temperature, the evolution of the density, the evolution of the liquid water content, and the onset of granulation and displays comparisons of these parameters.

3.4.1 Evolution of the snow temperature

The evolution of the snow temperature of the experiments with ambient air temperatures below 0 °C shows an interesting relation to the rotational speed.

In Figure 3.21 the snow temperatures (left) and correlating ambient air temperatures (right) for the fast experiments with approximately 15 rpm are displayed. It is observable that for quite similar air temperatures of approximately -5 ℃, the graphs of the snow temperatures are close to one another.
In Figure 3.22 the snow temperatures (left) and correlating ambient air temperatures (right) for the slow experiments with approximately 5.3 rpm are displayed. In the right Figure the ambient air temperatures of the experiments 240117_04 and 240117_05 are both around -4.5 ℃. The corresponding snow temperatures for these two slow experiments show a far higher deviation from one another than the snow temperatures in the fast experiments (Fig 3.21, left). Furthermore the evolution of the snow temperature for the experiment 170125_06 has by far the highest deviation from the other experiments in Figure 3.22 (left), but a comparison to the other experiments is difficult since the corresponding air temperature of this experiment is also approximately 4 ℃ warmer than in the other displayed experiments.

In Fig 3.23 the evolution of the snow temperature for the fast experiment 170123_02 is compared to the slow experiment 170124_04 (left) and the slow experiment 170124_05 (right). Mind that the evolution of the temperature is displayed over the travel distance of the flowing lobe in the vertically rotating drum. In both comparisons the slow experiments display a more rapid increase of the snow temperature related to the travel distance than the fast experiment.

For the warm experiments with air temperatures above or equal to 0 ℃ the snow heated up very quickly to 0 ℃, so that the evolutions of the snow temperature cannot be compared very well.

3.4.2 Evolution of the density

A comparison of the densities measured in every experiment is displayed in Figure 3.24. One can see that for the experiments where no granulation occurred (170123_01 – 170125_06), the density of the snow did not exceed 500 $\mathrm{kg\,m^{-3}}$.

For the experiments where granulation was observed (170125_07 – 170216_13) the densities of granules increased up to approximately 900 $\mathrm{kg\,m^{-3}}$. Especially for the experiments 170215_09 to 170216_13 the measurements are close to one another, regardless of the rotational velocity.

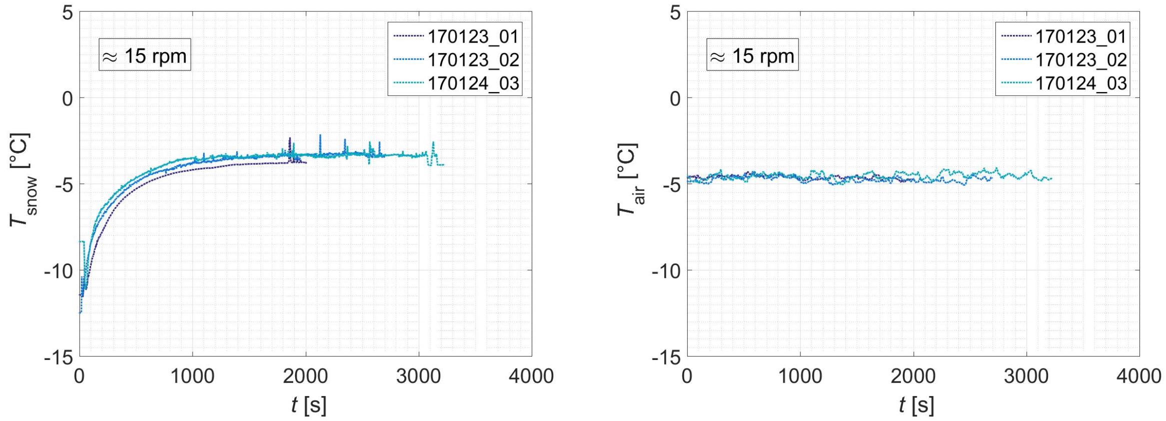

Figure 3.21: Evolution of the snow temperature (left) and air temperature (right) for experiments with ≈ 15 rpm and without the occurrence of granulation

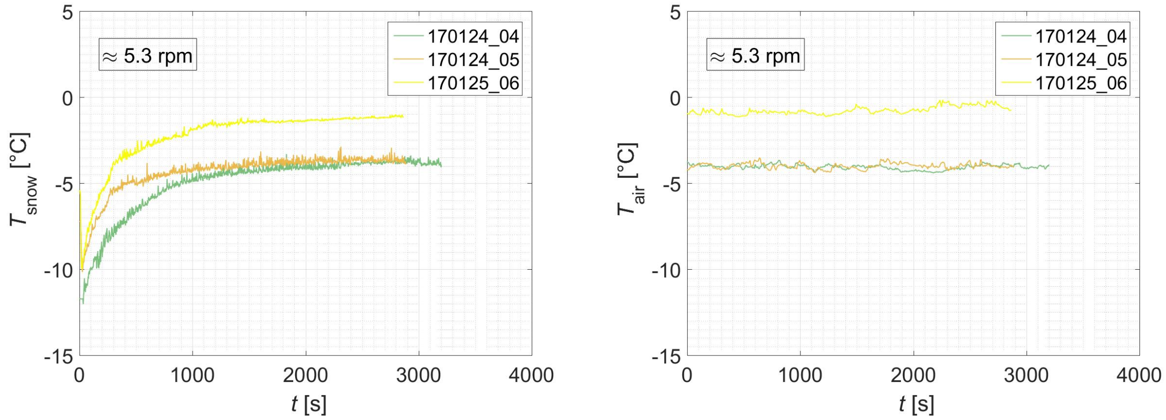

Figure 3.22: Evolution of the snow temperature (left) and air temperature (right) for experiments with ≈ 5.3 rpm and without the occurrence of granulation

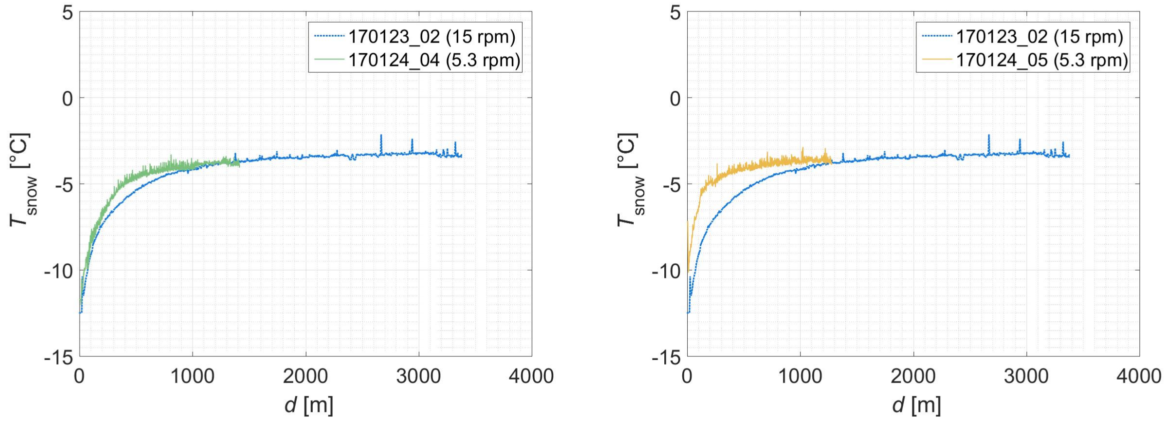

Figure 3.23: Evolution of the snow temperature with travel distance for experiment 170124_04 (left) and experiment 170124_05 (right) compared to experiment 170123_02.

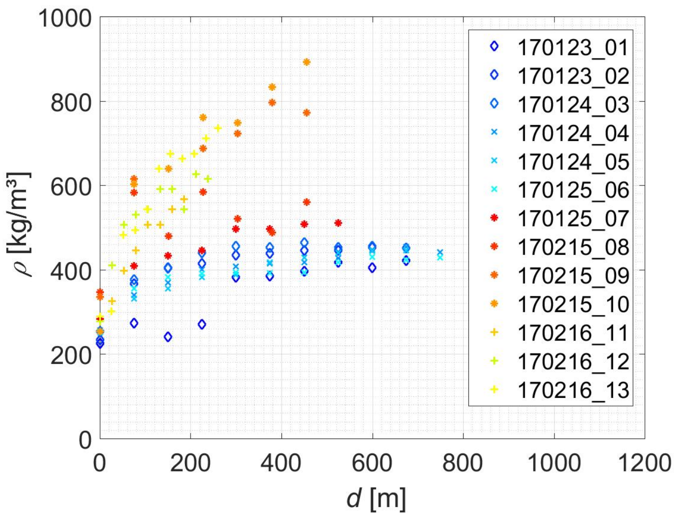

Figure 3.24: Evolution of the density with travel distance for all 13 experiments.

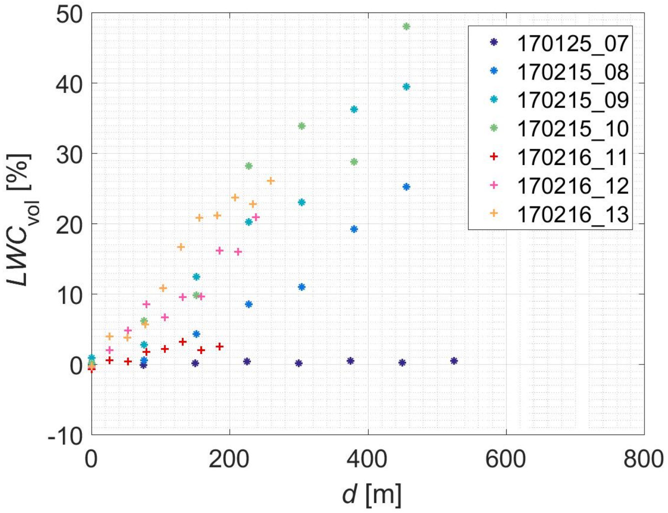

Figure 3.25: Evolution of the volumetric liquid water content with travel distance for the experiments where granulation occurred.

3.4.3 Evolution of the volumetric liquid water content

A comparison of the volumetric liquid water contents of all the experiments where granulation occurred (170125_07 – 170216_13) is shown in Figure 3.25. Apart from experiment 170125_07, where the volumetric liquid water content did not exceed 1 %, the measurements show an significant increase of free liquid water.

3.4.4 Onset of granulation

Out of the total variation of the normal pressure, the time when the granulation process initiated was determined. The physical parameters at the onset of granulation are listed in Table 3.2. These parameters were recorded at an interval of ± 10 s around the determined point in time where granulation initiated.

Furthermore Figure 3.26 illustrates the relation between the ambient air temperature (left) and the internal snow temperature (right) over the time until the onset of granulation. The data points represent the mean of the measurements in an interval of ± 10 s around the onset of granulation, and the vertical bars display their accuracy. For the ambient air temperature the measurements are very accurate, so the vertical bars are not very distinct in Figure 3.2, whereas for the internal snow temperature the bars for the accuracy could be plotted very well.

It can be observed that with increasing air temperature the time until occurrence of granulation mostly decreased, independent of rotation speed.

Table 3.2: Parameters at the onset of granulation: number of the experiment, rotational speed, time until the onset of granulation, ambient air temperature, snow temperature, and travel distance until the onset of granulation

experiment no.	f_{rot} [rpm]	t_{gran} [s]	$T_{\mathrm{air\_gran}}$ [°C]	$T_{\mathrm{snow\_gran}}$ [°C]	d_{gran} [m]
170125_07	15.0	955 ± 10	0.1 ± 0.1	-0.8 ± 0.2	1196 ± 13
170215_08	15.2	285 ± 10	6.6 ± 0.1	-0.1 ± 0.3	362 ± 13
170215_09	15.2	70 ± 10	7.3 ± 0.2	0.0 ± 0.2	89 ± 13
170215_10	15.2	65 ± 10	9.3 ± 0.2	0.0 ± 0.2	83 ± 13
170216_11	5.3	476 ± 10	3.3 ± 0.1	-0.6 ± 0.2	211 ± 4
170216_12	5.3	145 ± 10	4.7 ± 0.1	-0.2 ± 0.1	64 ± 4
170216_13	5.2	395 ± 10	4.8 ± 0.1	-0.4 ± 0.1	175 ± 4

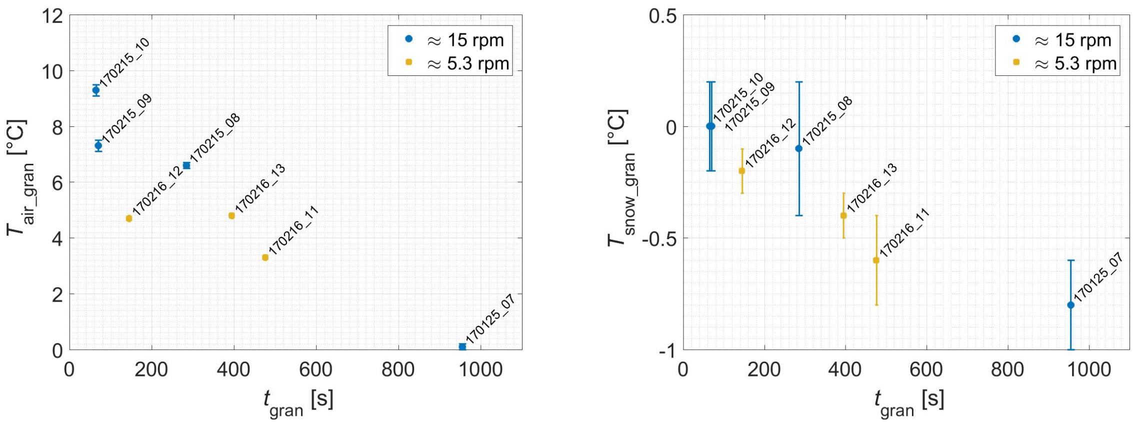

Figure 3.26: Time until the onset of granulation related to the ambient air temperature (left) and internal snow temperature (right). The mean of the measurements for an interval of $\pm\,10\,\mathrm{s}$ around the onset of granulation is displayed with vertical bars for the accuracy of the measurements.

4 Discussion

The flow behaviour of snow is investigated with a vertically rotating drum. This experimental set-up allows to observe the evolution of the physical properties of flowing snow over a long time.

4.1 Conducting the experiments

It is the first time that snow is investigated in a vertically rotating drum and the properties of the flowing material, such as temperature, density, and basal normal stress can be measured continuously over a long time. Since the experiments represent a new kind of method, several difficulties had to be encountered.

Usually the rotating drum is used indoor for the investigation of debris flows, where the ambient air temperature is of no specific interest. Since a part of the series of experiments with snow regard sub zero degree temperatures, the rotating drum was moved to an outdoor facility. After moving, the signal of the laser sensors and the force plates installed in the drum show an unusual high noise compared to their operation indoors. The cause for this noise is assumed to be the voltage regulator of the motor of the drum, but it could not be identified certainly. Further the measuring program and the data transfer are not running stable throughout the experiments. For a few experiments it freezes after some time and has to be restarted.

The noise in the signal is also accountable for the fact that the analysis of the data was not perfectly successful. Several outliers in the collected data made the evaluation very tricky and had to be excluded. This is represented for example in Fig 3.20 (left), where gaps in the displayed graph indicate the excluded outliers.

Another difficulty that was faced while conducting the experiments was the manual measurement of the density and liquid water content. For the loose snow sampling with the bailer worked very well, but it was nearly impossible to fill the bailer with granules without entrapping air. To measure the density of the granules anyway, cubes of known volume were cut out and their mass was scaled. To determine the dielectric permittivity of the snow, the prongs of the Decagon 5TM sensors had to be stuck into the snow. This again worked without any difficulty for the loose snow, but was very tough for the hard granules in order not to break the prongs.

4.2 Evaluation of the physical properties of snow

4.2.1 Evaluation of the density

The "cold" experiments below $-4\,°C$ display a rise of the density from initial $\approx 240\,\mathrm{kg\,m^{-3}}$ to final $\approx 450\,\mathrm{kg\,m^{-3}}$. One can observe in Figure 3.4 that the calculated density is up to $100\,\mathrm{kg\,m^{-3}}$ lower than the manually measured one. One possible explanation for the reduced calculated density could be that the snow measured moving in the drum is more fluidized than the snow measured in the bailer because the flow is more diluted due to constant shearing as described for granular and multi-phase flows by e.g. Forterre and Pouliquen (2008), Iverson and George (2014), or Bartelt and Buser (2016).

In the experiments at ambient air temperatures around $0\,°C$ as long as no granulation occurs, the calculated density is approximately $50\,\mathrm{kg\,m^{-3}}$ lower than the manually measured one. As displayed in the right graphic of 3.11, the calculated density drops significantly after granules start to form, while the manually measured density still continues rising. This discrepancy is because the bailer was filled with snow granules as void-free as possible to measure their density, while the granules in the flow had a lot of space between them. The calculated density out of the laser and force plate measurements is better referred to as the bulk density of the flow.

For "warm" experiments conducted at temperatures higher than $+4\,°C$, the calculated density drops with the onset of granulation (see Fig. 3.17, right). The evaluation of the calculated density on the left side of Fig. 3.17 not only has a big gap due to the malfunction of the data analysis, but also shows implausible results compared to all the other experiments where granulation occurred. If the analysis of the measured data were improved, the results would probably be in better accordance to the observations in the experiments.

A comparison of the evolution of all the densities throughout the experiments is displayed in Figure 3.24. It can be observed that in the experiments where no granulation occurred the density is significantly lower than in most of the experiments where the flowing snow formed granules. Especially densities above $600\,\mathrm{kg\,m^{-3}}$ are most likely a result of the relatively large amount of water in the snow, which is in accordance with the slush snow that was observed in the experiments. A further reason for this discrepancy can probably be found in the way the density was measured manually. For experiment 170123_01 to 170215_08 a sample was extracted with a bailer and weight to measure the density of the snow. For the experiments 170215_09 to 170216_13 it was not possible to fill the bailer without air entrapped between the granules. Therefore cubic samples with 5 cm side length were cut out of the granules and weight. This change of the measuring method might be a contributor to the significantly higher measurements of the density.

4.2.2 Evaluation of the temperature

In the experiments below -4 ℃, the temperature of the flowing snow increases significantly over the ambient air temperature for rotational speeds of approximately 15 rpm. At slow speeds (5.3 rpm) the rise of the temperature above the ambient air temperature can be observed as well, but it is considerable smaller in comparison with the fast experiments. This effect does not occur in the experiments around 0 ℃ and above $+4$ ℃, since the snow can only increase its temperature up to 0 ℃, and therefore cannot exceed the ambient air temperature.

It is shown in Figures 3.21 – 3.23 that the evolution of the snow temperature is different for different rotational speeds. Plotting the evolution of the snow temperature over the travel distance has the advantage that the amount of energy supplied by frictional heating is only depending on the travelled distance. Therefore in experiments with different rotational speeds the same amount of friction energy is put into the warming of the snow after the same travel distance. The difference in the comparison of slow and fast experiments illustrates that ambient heating plays a major role in the warming of the material in the drum.

The warming of the snow is subjected to frictional heating, heat conduction, heat radiation, and convective flow of heat. The physical equations to characterize this energy balance are very difficult since the process is close to the point of phase transformation.

Considering that in the experimental set-up snow entrainment is impossible, the energy to heat the snow above the ambient temperature must be obtained from shear work or the collisions of granules respectively, according to Vera Valero et al. (2012).

4.2.3 Evaluation of the liquid water content

The liquid water content is measured indirectly over the dielectric permittivity. The results show that liquid water only forms after the snow temperature reaches 0 ℃, which not only is in accordance with physics but also justifies the use of the Decagon 5TM sensor, which was originally designed for soil and not for snow.

As Figure 3.25 shows, in some of the experiments volumetric liquid water contents of 25 % and higher are measured, which is incredible high for wet snow avalanches and is rather associated with slush flows. A decrease of the static friction coefficient as proposed by Naaim et al. (2013) could not be measured since the rotating drum is not designed to investigate this kind of friction.

4.2.4 Evaluation of the onset of granulation

The onset of granulation takes place when the snow temperature is close to the melting point. The temperature threshold for the onset of granulation at − 1 ℃ as proposed by Steinkogler et al. (2014) can not be confirmed precisely. As Figure 3.26 (right) illustrates, the internal snow temperatures at the initiation of granulation are all above − 1 ℃. Some of the measured snow temperatures even exceed 0 ℃, which is physically not possible and a clear effect of the uncertainty of measurement.

To describe the correlation between the ambient air temperature and the time until the onset of granulation, as displayed in Figure 3.26 (left), with a formula or evaluate it statistically, more experiments have to be conducted to support the investigation with a bigger data base. With the currently available data records, any correlation from linear to logarithmic proportionality could be possible.

Since the liquid water content is not measured continuously in the conducted experiments, consequently the exact amount of free liquid water in the snow when granulation starts can not be distinguished out of the measurements. However it can be observed that no granulation occurs as long as the is no free liquid water available.

Further the videos of the flow allow to derive the grain size distribution. It was not the aim of this thesis to analyse the grain size distribution, but a method has been developed to look into that as well. In the video frames of the granulation process polygons are drawn encircling the single granules. With suitable software the dimensions of the grains are measured and a particle size distribution curve is generated. If this is applied to frames with defined time intervals the evolution of the grain size distribution can be investigated.

4.3 Answers to the research questions

- **What are the relevant experimental properties and how do they influence what is observed in the experiments?**
  The general flow behaviour that is observed while conducting the experiments is mostly dependent on the snow temperature and on the rotational speed. The air temperature is a major contributor of thermal energy to the flowing material but can not be adjusted at will. Only the time can be chosen at which the experiments are conducted, so that the air temperature fits the purpose of the investigation. The rotational speed accounts for the dissipation of energy through shear forces and friction. The higher the velocity, the more frictional energy is available to warm the flowing snow.

  The flow can mostly be regarded as steady in the reference system of the laboratory, since the flow velocity in the drum is mainly constant. Some of the physical properties like the flow height, the density, and the appearance of the flowing material (loose snow, granules) change throughout the experiment. The flow behaviour can be described through the following three types that prevail exclusively, but can appear consecutively or alternately:

  - The flow is steady and consists of loose snow or granules respectively with internal deformation. The front of the flowing lobe is constantly at the same position while the flow height decreases and the density increases slowly. This is called the steady flow behaviour.
  - The flowing material sticks to the basal sliding surface and gets transported as a bulk up to the wiper where it accumulates. When the static friction is overcome, the bulk slides downwards and sticks to the basal surface again. This appears both for loose snow and granules and is called the stick-slip flow behaviour.
  - After the onset of granulation a composition of loose snow and granules prevails, until all the loose snow has evolved into granules. With this composition internal shearing in the lobe can be observed. Shortly after the granulation process is finished, the internal deformation stops and the entire body consisting out of granules moves as a bulk with a highly sheared sliding plane.

- **How do the flow measurement quantities evolve during time?**
The volumetric liquid water content is 0 % when the temperature of the snow is below the melting point. As soon as the snow has 0 ℃, free liquid water starts to form and therefore the volumetric liquid water content starts to increase. In the conducted experiments values between 0 % and 48 % are measured, although the majority of the experiments does not exceed volumetric liquid water contents higher than approximately 25 %. Only in two experiments (170215_09 & 170215_10) slushy snow forms that has very high (40 % and 48 % resp.) final liquid water contents.

  The snow temperature throughout the experiments is mostly depending on the ambient air temperature and the rotational speed. For ambient temperatures below − 4 ℃ the snow temperature rises significantly above the air temperature in the experiments with ≈ 15 rpm and only slightly for experiments with ≈ 5.3 rpm. For ambient temperatures around 0 ℃ and above, the snow temperature increases to 0 ℃ and the phase transformation from solid to liquid starts.

  In all the conducted experiments the density of the flowing snow increases. If the flow consists out of loose snow throughout the whole experiment, the actual snow density and the flowing bulk density display the same behaviour. In contrast, when granules form, their density differs a lot from the flowing bulk density, because a lot of air is between the granules moving in the drum.

- **Is there some direct connection between the evolution of the snow temperature and the onset of granulation?**
Yes. The granulation starts after the snow temperature exceeds approximately − 1 ℃. This can be observed in all the conducted experiments. To describe the correlation between the snow temperature and the initiation of granulation more precisely, the investigation should be supported by a bigger data base.

- **Is there some direct connection between the liquid water content and onset of granulation?**
Probably. Since the liquid water content was measured in intervals of 300 s and not continuously, a direct connection can not be verified with the experimental set-up. But the results implicate that the formation of free liquid water and the onset of granulation correlate.

5 Conclusions

In this work I present experiments on the flow behaviour of snow in a vertically rotating drum. The aim of this study was to test a new method to investigate flowing snow and the evolution of its physical properties over a longer time period.
The results show that the vertically rotating drum is an applicable technique to examine the flow behaviour of snow. The instrumental set-up included laser sensors for the flow height, load cells for the basal normal pressure, temperature couples for the snow and ambient air temperature, a dielectric sensor for the permittivity of the snow, a video camera, and a torque gauge for the torque at the driving shaft. For the experiments presented in this work, not all of the possibilities to gain measurements of the flowing material were exploited or evaluated and the drum has the potential to offer many more.

The evolution of the snow temperature and the formation of granules could be observed very well in the rotating drum. The energy dissipation of the flowing material was depending on the rotational speed of the drum, and the snow could even warm above the ambient temperatures if the drum rotates fast enough. Further the data support that the snow temperature of $-1\,^{\circ}\mathrm{C}$ plays a critical role for the onset of granulation.

Some difficulties while conducting the experiments as well as in the evaluation of the data had to be encountered, but the main weakness of the work was in the analysis of the data measured by laser and normal pressure sensors. To provide better results for further calculations (e.g. density) this analysis needs to be improved.

Future research on the flow behaviour of snow in the vertically rotating drum could contribute a comprehensive consideration of the energy balance of the flow to improve the general understanding and enhance physical modelling.

Bibliography

Ambach, W., Denoth, A., 1975. On the Dielectric Constant of Wet Snow. Snow Mechanics Symposium; Proceedings of the Grindelwald Symposium; International Association of Hydrological Sciences Publication No. 114, p 136-142 (Journal Article).

Baggi, S., Schweizer, J., Jul. 2009. Characteristics of wet-snow avalanche activity: 20 years of observations from a high alpine valley (Dischma, Switzerland). Natural Hazards 50 (1), 97–108.

Bartelt, P., Buser, O., Jun. 2016. The relation between dilatancy, effective stress and dispersive pressure in granular avalanches. Acta Geotechnica 11 (3), 549–557.

Bartelt, P., McArdell, B. W., Dec. 2009. Granulometric investigations of snow avalanches. Journal of Glaciology 55 (193), 829–833.

Brun, E., Rey, L., 1987. Field study on snow mechanical properties with special regard to liquid water content. International Association of Hydrological Sciences Publication 162, 183–193.

Colbeck, S. C., 1987. Snow Metamorphism and Classification. In: Jones, H. G., Orville-Thomas, W. J. (Eds.), Seasonal Snowcovers: Physics, Chemistry, Hydrology. Springer Netherlands, Dordrecht, pp. 1–35.

De Biagi, V., Chiaia, B., Frigo, B., 2012. Fractal grain distribution in snow avalanche deposits. Journal of Glaciology 58 (208), 340–346.

Denoth, A., Jan. 1989. Snow dielectric measurements. Advances in Space Research 9 (1), 233–243.

Denoth, A., 1994. An electronic device for long-term snow wetness recording. Annals of Glaciology 19, 104–106.

Denoth, A., Foglar, A., Weiland, P., Mätzler, C., Aebischer, H., Tiuri, M., Sihvola, A., Oct. 1984. A comparative study of instruments for measuring the liquid water content of snow. Journal of Applied Physics 56 (7), 2154–2160.

Fierz, C., Armstrong, R. L., Durand, Y., Etchevers, P., Greene, E., McClung, D. M., Nishimura, K., Satyawali, P. K., Sokratov, S. A., 2009. The International Classification for Seasonal Snow on the Ground. Vol. 25. UNESCO/IHP Paris.

Forterre, Y., Pouliquen, O., Jan. 2008. Flows of Dense Granular Media. Annual Review of Fluid Mechanics 40 (1), 1–24.

Frolov, A. D., Ya. Macheret, Y., Sep. 1999. On dielectric properties of dry and wet snow. Hydrological Processes 13 (12-13), 1755–1760.

Gauer, P., Issler, D., Lied, K., Kristensen, K., Sandersen, F., 2008. On snow avalanche flow regimes: Inferences from observations and measurements. In: Proceedings Whistler 2008 International Snow Science Workshop September 21-27, 2008. p. 717.

Iverson, R. M., George, D. L., Jul. 2014. A depth-averaged debris-flow model that includes the effects of evolving dilatancy. I. Physical basis. Proceedings of the Royal Society A: Mathematical, Physical and Engineering Sciences 470 (2170), 20130819–20130819.

Kaitna, R., Rickenmann, D., Schatzmann, M., Jul. 2007. Experimental study on rheologic behaviour of debris flow material. Acta Geotechnica 2 (2), 71–85.

Kern, M., Tiefenbacher, F., McElwaine, J., Oct. 2004. The rheology of snow in large chute flows. Cold Regions Science and Technology 39 (2-3), 181–192.

Kobayashi, T., Nohguchi, Y., Izumi, K., 2000. Comparison of dry granulation and wet agglomeration of snow. Snow engineering : recent advances and developments : proceedings of the Fourth International Conference on Snow Engineering, 93–97.

McClung, D., Schaerer, P. A., 2006. The Avalanche Handbook, 3rd Edition. Mountaineers Books, Seattle, WA, oCLC: ocm70176894.

McClung, D. M., Schaerer, P. A., 1985. Characteristics of Flowing Snow and Avalanche Impact Pressures. Annals of Glaciology 6, 9–14.

Mitterer, C., 2012. Formation of wet-snow avalanches. Ph.D. thesis, ETH Zurich.

Mitterer, C., Schweizer, J., Feb. 2013. Analysis of the snow-atmosphere energy balance during wet-snow instabilities and implications for avalanche prediction. The Cryosphere 7 (1), 205–216.

Naaim, M., Durand, Y., Eckert, N., Chambon, G., Aug. 2013. Dense avalanche friction coefficients: Influence of physical properties of snow. Journal of Glaciology 59 (216), 771–782.

Prenner, D., 2011. Erstellung eines automatisierten Auswertetools für Labormessdaten. Bachelor Thesis at the University of Life Sciences and Natural Ressources, Vienna.

Schaefer, M., Bugnion, L., Jun. 2013. Velocity profile variations in granular flows with changing boundary conditions: Insights from experiments. Physics of Fluids 25 (6), 063303.

Sovilla, B., Bartelt, P., 2002. Observations and modelling of snow avalanche entrainment. Natural Hazards and Earth System Science 2 (3/4), 169–179.

Sovilla, B., Margreth, S., Bartelt, P., Jan. 2007. On snow entrainment in avalanche dynamics calculations. Cold Regions Science and Technology 47 (1-2), 69–79.

Sovilla, B., Schaer, M., Kern, M., Bartelt, P., Feb. 2008. Impact pressures and flow regimes in dense snow avalanches observed at the Vallée de la Sionne test site. Journal of Geophysical Research 113 (F1).

Steinkogler, W., Gaume, J., Löwe, H., Sovilla, B., Lehning, M., Jun. 2015. Granulation of snow: From tumbler experiments to discrete element simulations. Journal of Geophysical Research: Earth Surface 120 (6), 1107–1126.

Steinkogler, W., Sovilla, B., Lehning, M., Jan. 2014. Influence of snow cover properties on avalanche dynamics. Cold Regions Science and Technology 97, 121–131.

Techel, F., Pielmeier, C., May 2011. Point observations of liquid water content in wet snow – investigating methodical, spatial and temporal aspects. The Cryosphere 5 (2), 405–418.

Vera Valero, C., Feistl, T., Steinkogler, W., Buser, O., Bartelt, P., 2012. Thermal temperature in avalanche flow. In: Proceedings Anchorage 2012 International Snow Science Workshop September 16-21, 2012. p. 32.

Appendix

Figure A.0: Photograph of the rotating drum with scientists for scale

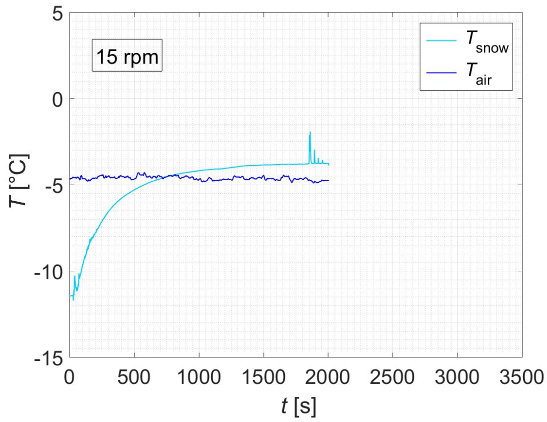

Figure A.1: Experiment 170123_01: evolution of the snow and air temperature

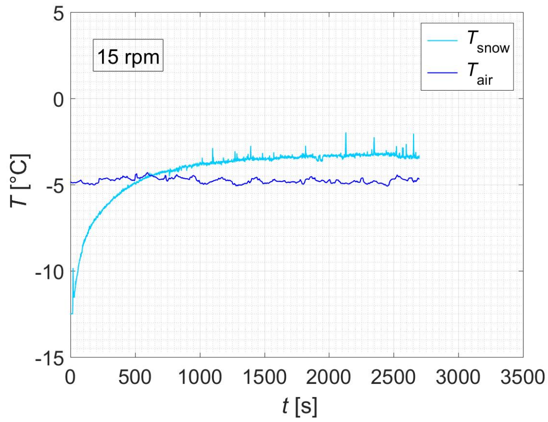

Figure A.2: Experiment 170123_02: evolution of the snow and air temperature

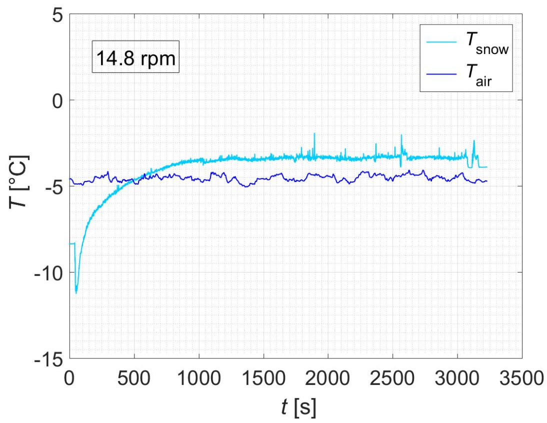

Figure A.3: Experiment 170124_03: evolution of the snow and air temperature

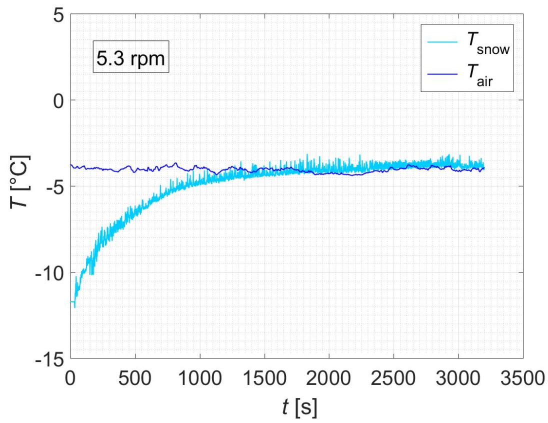

Figure A.4: Experiment 170124_04: evolution of the snow and air temperature

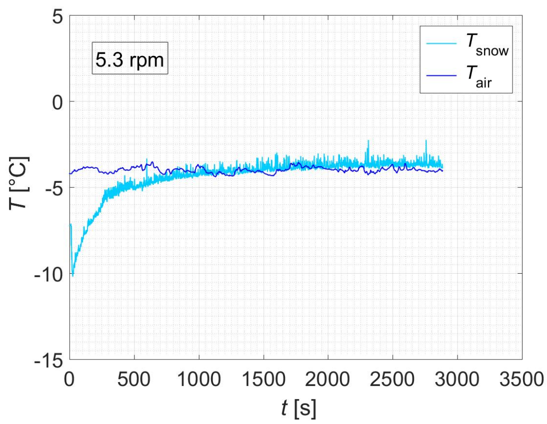

Figure A.5: Experiment 170124_05: evolution of the snow and air temperature

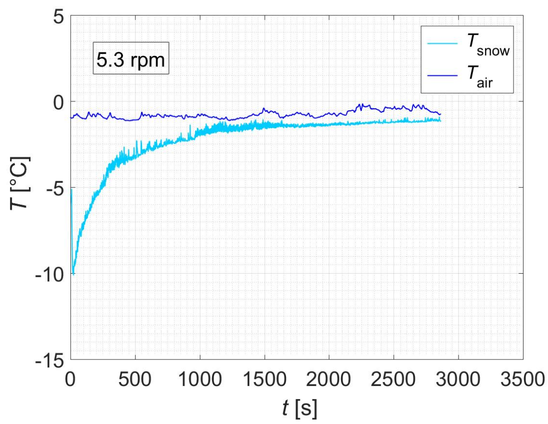

Figure A.6: Experiment 170125_06: evolution of the snow and air temperature

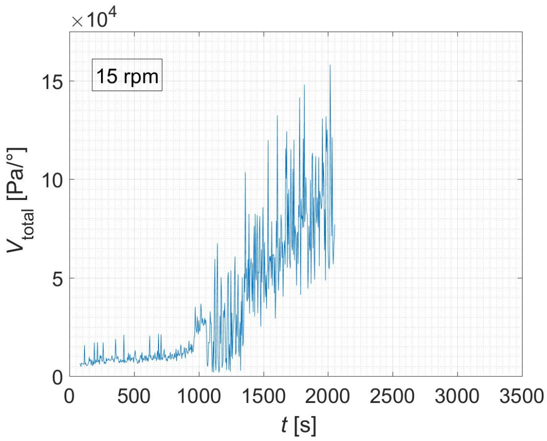

Figure A.7: Experiment 170125_07: Total variation of the normal pressure

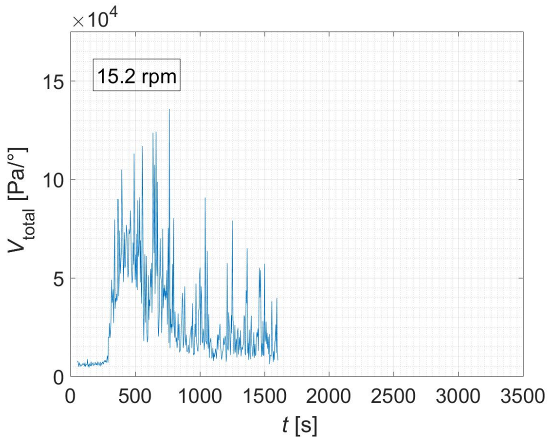

Figure A.8: Experiment 170215_08: Total variation of the normal pressure

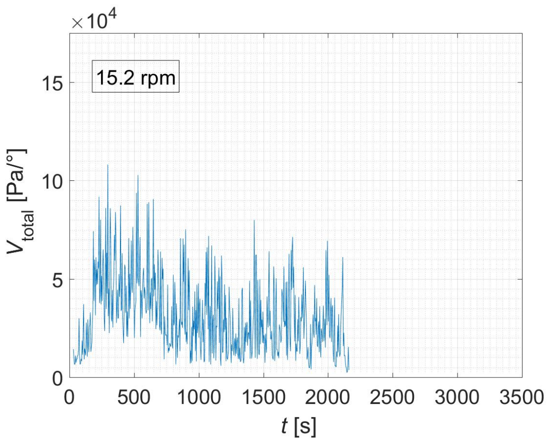

Figure A.9: Experiment 170215_09: Total variation of the normal pressure

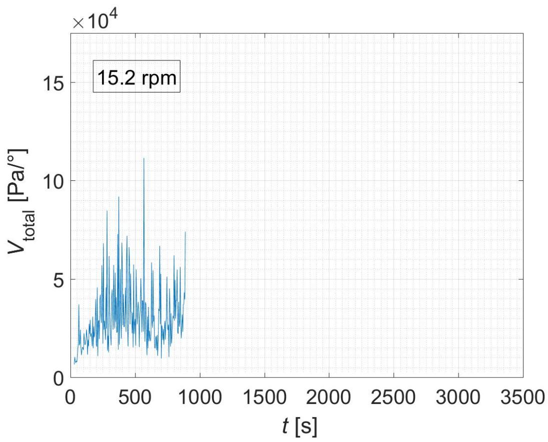

Figure A.10: Experiment 170215_10: Total variation of the normal pressure

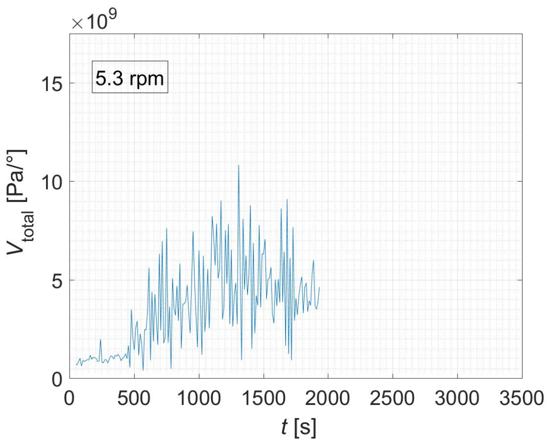

Figure A.11: Experiment 170216_11: Total variation of the normal pressure

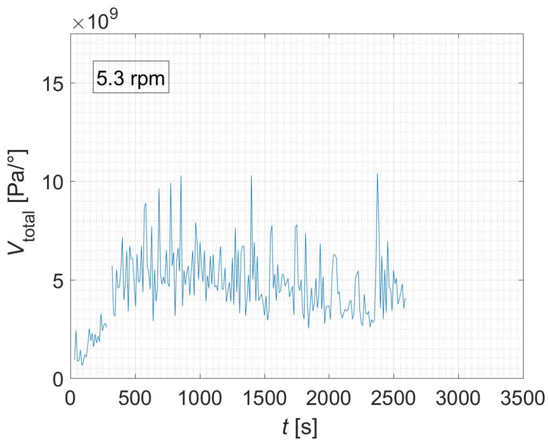

Figure A.12: Experiment 170216_12: Total variation of the normal pressure

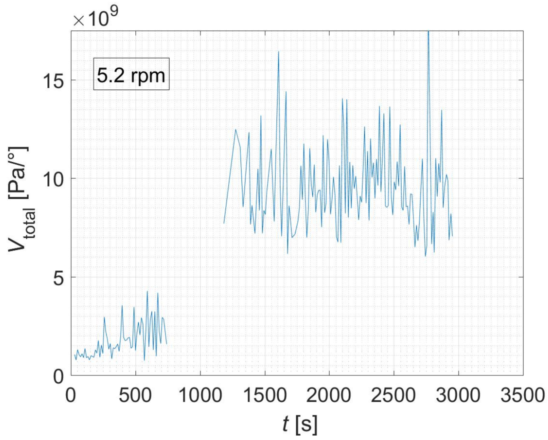

Figure A.13: Experiment 170216_13: Total variation of the normal pressure

List of Figures

List of Tables

List of Abbreviations

ε = dielectric permittivity [ ]
ε' = real part of the dielectric permittivity [ ]
ε'' = imaginary part of the dielectric permittivity [ ]
ε_{r} = relative permittivity [ ]
ε_0 = dielectric constant [ ]
$\varepsilon'_{\mathrm{air}}$ = dielectric permittivity of air [ ]
$\varepsilon'_{\mathrm{ice}}$ = dielectric permittivity of ice [ ]
$\varepsilon'_{\mathrm{water}}$ = dielectric permittivity of water [ ]
θ_{COG} = deviation angle [°]
λ = wavelength [nm]
ν = frequency [Hz]
ρ = density [$\mathrm{kg\,m^{-3}}$]
ρ_{calc} = calculated density [$\mathrm{kg\,m^{-3}}$]
ρ_{rel} = density relative to the density of water [ ]
φ = angle [°]
d = travel distance of the material [m]
d_{gran} = travel distance until the onset of granulation [m]
f_{rot} = rotational speed [rpm]
g = gravitational acceleration [$\mathrm{m\,s^{-2}}$]
h = flow height [m]
k = sensor-specific calibration factor for the Denoth-Meter [ ]
LWC_{vol} = volumetric liquid water content [%]
LWC_{m} = liquid water content per mass [%]
p = normal pressure [Pa]
r = radius of the drum [m]
t = time [s]
T_{air} = temperature of the air [°C]
$T_{\mathrm{air\_gran}}$ = temperature of the air at the onset of granulation [°C]

t_{gran} = time until the onset of granulation [s]
T_{snow} = temperature of the snow [℃]
T_{snow_gran} = temperature of the snow at the onset of granulation [℃]
U = bridge voltage at the Denoth-Meter with sensor in snow [V]
U_{ref} = bridge voltage at the Denoth-Meter with sensor in cool air [V]
V_{total} = total variation [Pa/°]